José Manuel Domínguez-Esquivel
Manuel Ramos   *Editors*

Advanced Catalytic Materials: Current Status and Future Progress

Springer

José Manuel Domínguez-Esquivel
Manuel Ramos

Editors

Advanced Catalytic Materials: Current Status and Future Progress

🐎 Springer

Chapter 4
Catalytic Materials for Hydrodesulfurization Processes, Experimental Strategies to Improve Their Performance

Jorge Ramírez, Perla Castillo-Villalón, Aída Gutiérrez-Alejandre, Rogelio Cuevas, and Aline Villarreal

4.1 Introduction

The production of clean liquid transport fuels requires highly active hydrodesulfurization catalytic materials to achieve the set goals of low sulfur content in accordance with worldwide environmental regulations that are pushing the limits for nearly zero ppm of sulfur content in liquid fuels. The increasing use of feedstocks with low quality, which contain higher concentrations of sulfur, nitrogen, metals, and other contaminants, creates heavier demands on the catalytic materials used for hydrodesulfurization, which must eliminate larger amounts of organic sulfur compounds of low reactivity and other nitrogen compounds that inhibit hydrodesulfurization and hydrogenation reactions.

The removal of sulfur from molecules of low reactivity takes place by two main reaction routes: the direct desulfurization (DDS) and hydrogenation (HY). In that sense, it is necessary to achieve a good understanding of the nature and chemical behavior of the different active sites in the catalytic material, and of the factors that influence activity and selectivity, concerning both direct desulfurization and hydrogenation catalyst functionalities.

Most hydrodesulfurization catalytic materials are composed of MoS_2 crystallites with addition of cobalt or nickel (Co, Ni) atoms to comprise a sulfide phase. For commercial applications, due to high pressure and temperature reaction conditions, the Co(Ni)Mo sulfide phase is usually supported on alumina oxide (Al_2O_3), as well described by Topsøe et al. [1].

J. Ramírez (✉) · P. Castillo-Villalón · A. Gutiérrez-Alejandre · R. Cuevas · A. Villarreal
UNICAT, Departamento de Ingeniería Química, Facultad de Química, UNAM, CDMX, Mexico
e-mail: jrs@unam.mx

Experimental and theoretical evidence points out that active sites for sulfur removal are located at sulfur vacancies at MoS_2 crystallite edges. Therefore, the overall HDS reaction is structure sensitive in principle and the activity of the catalytic material will be dependent on the crystallite size and edge termination as presented using theoretical density functional theory-based studies by different research groups [2–9]. Moreover, Lauritsen et al. presented a study using scanning tunneling microscopy (STM) contrasted with computer-assisted DFT simulations to determine the location of the Co promoter on MoS_2 low-size slabs, allowing the understanding of "brim sites," providing better knowledge of the catalytic material [10, 11].

Furthermore, the same group lead by H. Topsøe achieved one STM study to determine any chemical interaction of sterically hindered dibenzothiophenes using same triangular cobalt-promoted MoS_2 model particles under ultrahigh-vacuum operational conditions. Dibenzothiophene (DBT), which is mainly used to test at laboratory scale HDS catalytic materials, was adsorbed at edge sites located near corners of the MoS_2 triangular nanostructure whereas the adsorption of 4,6-dimethyldibenzothiophene, which is a sterically hindered molecule, and is mainly transformed through the hydrogenation route, took place on the so-called brim sites located near the edge at MoS_2 crystallites [12]. These results suggested a two-site reaction model for HDS of 4,6-DMDBT to occur, composed of hydrogenation of the first aromatic ring taking place at brim sites and subsequent sulfur removal of the hydrogenated intermediate at sulfur vacancies at the edge of the MoS_2 particle. The optimization of a catalyst depends then on the rate-controlling step in the sequence of reactions.

Now, sulfur molecules present in the different liquid fuels obtained from crude oil can display different reactivity and complex chemical structures, making important a high-quality design of HDS catalytic materials. For example, to obtain ultralow sulfur diesel one must eliminate sulfur from refractory molecules like 4,6-DMDBT and therefore the hydrogenating functionality of the catalytic material should be enhanced because those molecules react mainly through the hydrogenation reaction routes; in other words, a catalyst with a high hydrogenation/desulfurization selectivity is necessary to achieve good catalytic performance. On the contrary, for the hydrodesulfurization of fluid catalytic cracking (FCC) liquid gasoline, which contains sulfur aromatic compounds such as thiophenes and benzothiophenes, a low hydrogenation/desulfurization selectivity is required in the catalytic material to enhance the direct desulfurization route and inhibit deep hydrogenation, avoiding in this way olefin saturation, which is the main cause of hydrogen consumption and octane loss, with economic benefits.

When the feed is mixed with low-value fractions, as occurs for diesel production where sometimes light cycle oil is added to the feed, the catalyst must eliminate sulfur in the presence of high concentrations of nitrogen and aromatic compounds, which are poisons to both the hydrogenating and direct desulfurization sites of the catalyst. From theoretical studies made using DFT methods, it was possible to determine that basic heterocyclic nitrogen compounds strongly inhibit the hydrogenation route for HDS, which is the key step for achieving ultralow sulfur diesel,

because the elimination of the most refractory sulfur-containing molecules like 4,6-DMDBT is necessary, which mainly occurs through the hydrogenation routes [13].

The nature of the support matrix, mainly composed in commercial catalysts by alumina oxides (Al_2O_3), can have great influence in the performance of the hydrotreating catalyst. A support matrix with high chemical interaction allows uniform dispersion of the cobalt, nickel, and molybdenum precursor phases; however, it can be detrimental to the degree of sulfidation of the final Ni- and Co-promoted MoS_2 nanoclusters. Some experimental studies using X-ray photoelectron spectroscopy (XPS) indicate electronic binding of oxygen species from the Al_2O_3 complex matrix and molybdenum, which mainly occurs during the calcination process and remains after the sulfidation step, made with hydrogen disulfide (H_2S), giving rise to the presence of oxysulfides in the final catalytic material. These partially sulfided structures have low catalytic activity and have been named type I Co(Ni)-Mo-S whereas the well-sulfided ones displaying high HDS activity have been named type II Co(Ni)MoS structures [14]. A density functional theory study made to investigate the origin of the activity differences between type I and type II MoS_2-based structures in hydrotreating catalysts showed that indeed the presence of bridging oxygen bonds between molybdenum and support matrix modifies the electronic properties of the MoS_2-supported phase [9].

Experimental evidence shows that the adequate choice of the catalytic support is important since its chemical nature regulates the interaction between the Mo and Co (or Ni) phases with the support matrix surface, playing an important role to achieve high dispersion, sulfidation, and promotion of the MoS_2 nanoclusters and finally high HDS activity in the transformation of complex organic sulfur molecules as those present in crude oil. In our research group, some strategies used to prepare highly active HDS catalysts consist of optimizing dispersion, sulfidation, and promotion of the MoS_2 nanoclusters by using different supports, organic additives like EDTA or citric acid, Mo and Co(Ni) heteropolycompounds as precursor salts, and modification of the sulfidation methodology. In what follows some work performed using these strategies is outlined.

4.2 Choice of the Catalyst Support

Experimental studies made by us revealed that the composition of the catalyst support matrix has an important effect on the dispersion of the active phase and plays an important role in the extent of promotion and sometimes in the intrinsic activity of Mo- and Co-promoted Mo sulfide particles [15, 16] improving HDS catalyst performance.

With the aim of improving the performance of HDS catalysts, to produce ultralow sulfur fuels, support materials with different metal-support interaction strength have been tried during the past years [17–19]. Benefits in HDS activity for catalysts using many different supports such as titanium dioxide (TiO_2), zirconium dioxide (ZrO_2), magnesium oxide (MgO), pristine forms of carbon, cerium oxide (CeO_2), silicon

oxide (SiO_2), zeolites, MCM-41, SBA-15, natural mineral clays, and various mixed oxides, TiO_2–Al_2O_3, among others, have been reported. For more information, we invite the reader to revise Ramirez et al. [16].

Earlier, Ramírez et al. [15] reported that the turnover frequency in thiophene HDS is about 4.4 times higher for titania-supported than for γ-alumina-supported MoS_2. To explain this important finding, electronic effects [15], orientation effects [20], and promotion by Ti [21–23] have been proposed in the past. Theoretical methods such as density functional theory (DFT) simulations have also been tried to understand the structure and behavior of HDS catalysts supported on different materials such as γ-Al_2O_3 or TiO_2 [24].

In a study that combined thiophene HDS activity and X-ray photoelectron spectroscopy on flat model systems of sulfided HDS Mo catalysts, Coulier et al. [23] found that the sulfided Ti species can act as a promoter in the same way as Co and Ni, although less effectively, confirming the original proposal of Ramírez et al. [21]. The fact that Ti in TiO_2 can act as an electronic promoter of the supported MoS_2 explains the higher thiophene HDS activity and hydrogenation selectivity of Mo/TiO_2 compared with Mo/Al_2O_3.

Another experimental study targeting at the effects of cobalt and nickel promoters for molybdenum disulfide catalysts supported either on Al_2O_3 or TiO_2 reported on the hydrodesulfurization of thiophene (T), dibenzothiophene (DBT), and 4,6-dimethyldibenzothiophene (4,6-DMDBT) [25]. The study, that comprised different catalytic supports (TiO_2 and Al_2O_3) and reacting molecules (thiophene, dibenzothiophene, and 4,6-DMSBT), showed that the greater activity displayed by Mo/TiO_2 compared to Mo/Al_2O_3 comes from a moderate increase in the direct desulfurization capability but mostly from an increase in the hydrogenating character of the catalyst due to the enhanced MoS_2 metallic character induced by TiO_2, showing that not only the overall HDS activity but also the HYD/DDS selectivity can be significantly influenced by the nature of the catalytic support matrix. The hydrodesulfurization rate constants for thiophene (T), dibenzothiophene (DBT), and 4,6-dimethyldibenzothiophene (4,6-DMDBT) over Mo, CoMo, and NiMo catalysts supported on TiO_2 and Al_2O_3 are displayed in Fig. 4.1 that shows that for the unpromoted catalysts there is a clear advantage in using titania instead of alumina as matrix support, MoS_2 supported on titania being 4, 4.4, and 2.7 times more active in the hydrodesulfurization of thiophene (T), dibenzothiophene (DBT), and 4,6-dimethyldibenzothiophene (4,6-DMDBT), respectively. However, promoted systems display a different behavior. The magnitude of the promotional effect varies with the reacting molecule and seems to be more effective when the reacting molecule is transformed through the direct desulfurization route, as in the case of thiophene and DBT. In contrast, for the hydrodesulfurization of 4,6-DMDBT, that takes place mainly via the hydrogenation route, the promotional effect for Co(Ni)Mo/TiO_2 is not observed, in spite of the fact that Mo/TiO_2 is 2.75 times more active than Mo/Al_2O_3, suggesting that the promotion effect expected from Co or Ni was already achieved by the use of titania as support matrix.

For thiophene and DBT that undergo HDS mainly by the direct desulfurization route, the promotional effect of Co or Ni for the TiO_2-supported catalysts is clearly
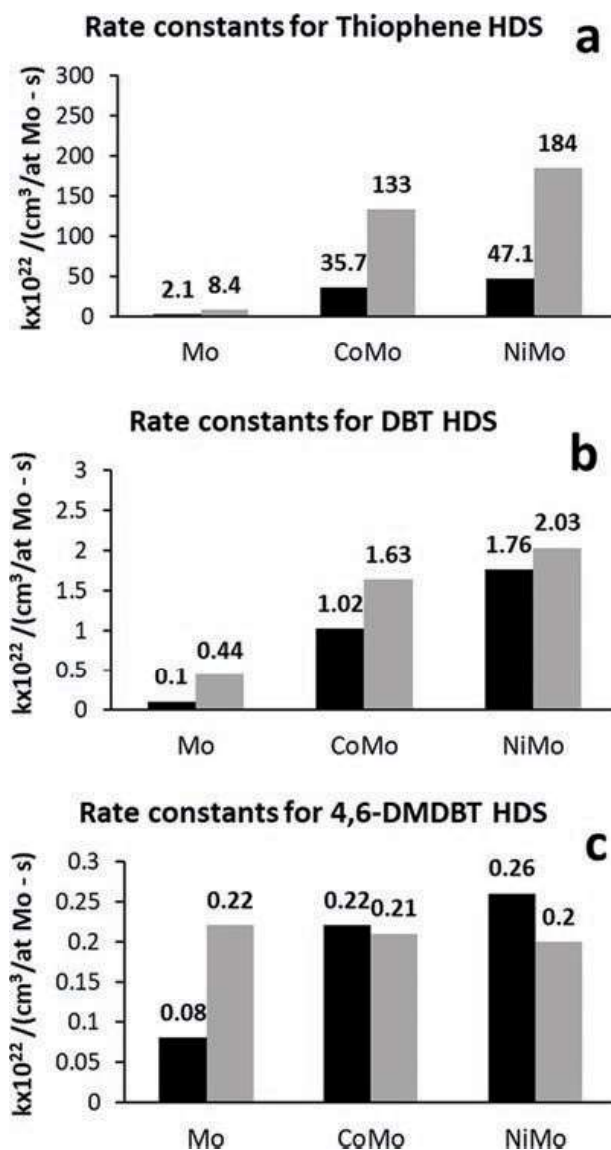
Fig. 4.1 Overall rate constant for the HDS of (**a**) thiophene, (**b**) dibenzothiophene, and (**c**) 4,6-dimethyldibenzothiophene over Mo, CoMo, and NiMo catalysts supported on Al_2O_3 and TiO_2. Extracted from [25] with permission from Elsevier

observed: ≈16 times for thiophene and ≈3.7 times for DBT. Therefore, enhancement of catalytic activity when using TiO_2 support matrix seems to be more effective for direct desulfurization reactions.

In the case of Al_2O_3-supported MoS_2, the promotional effects of Co or Ni are clearly observed during HDS laboratory test runs for the three different reactant molecules, and are much higher than those observed for TiO_2-supported catalysts.

In the past we postulated that under HDS reaction conditions (high H_2 pressure and temperature) TiO_2 could act as an electronic promoter [22], as found in an experimental temperature-programmed reduction study of the sulfided materials (TPR-S) made by Ramírez et al. [21]. The study showed that the number of

coordinatively unsaturated sites (CUS), or sulfur vacancies, per Mo atom increased with the Ti content. It was proposed that the increased number of sulfur vacancies in the catalyst would be the result of an electronic promotion of Mo by Ti causing the weakening of the Mo–S bond due to injection of electrons, coming from Ti^{3+} centers, to the HOMO of Mo, occupying antibonding orbitals.

The fact that the promotion either with Ni or Co is smaller for Mo/TiO_2 than for Mo/Al_2O_3 systems [25] suggests that either the Mo species supported on TiO_2 are more difficult to promote than those supported over alumina matrix or the optimum value of the Mo–S bond energy was not reached with the electronic promotion of Ti, and that some additional promotion coming from Ni or Co is required to achieve the value of the metal–sulfur bond energy that optimizes the interaction between the sulfur organic compound and the CUS active site. The electronic promotion must have a limit, or a maximum according to the Sabatier principle, as explained by Chianelli et al. for transition metal sulfides [26], because excessive weakening of the metal sulfur bonds in MoS_2 would lead to an excessively weak interaction between the sulfur compounds and the active phase. The results reported by Ramírez et al. [27], showing that the reduction of Mo or W oxide phases supported on pure TiO_2 or TiO_2–Al_2O_3 materials takes place at lower temperatures than for pure alumina-supported systems, are in agreement with the above explanation.

DFT investigations comparing the thermodynamic stability of MoS_2 particles anchored by S edge and Mo edge on alumina and titania under HDS conditions were presented by Costa et al. [28]. It was proposed that an edge-wetting effect present in Mo/TiO_2 and not in Mo/Al_2O_3 is at the origin of the smaller MoS_2 particles found for supported Mo on TiO_2. Their results indicated that at HDS conditions MoS_2 particles supported on anatase are edge-on with a trapezoidal shape exposing only one sulfur edge and two Mo edges. However, the higher dispersion achieved by the smaller particles is partly compensated by the number of Mo atoms buried in the MoS_2-anatase interphase (two sulfur edges and one Mo edge). Therefore, the number of exposed sulfur edge Mo atoms does not increase sufficiently to explain the fourfold increase in thiophene HDS activity observed experimentally. Since the variation in edge dispersion did not account for the observed results, an explanation related to the intrinsic nature of the catalytic site was proposed.

Recently, Castillo-Villalón et al. [25] found experimentally, by CO adsorption analyzed by FTIR spectroscopy, that the promotion of Mo by Co is more difficult when Mo is supported on TiO_2 than when supported on Al_2O_3. Thus, the number of promoted sites in CoMo supported on alumina is much higher than when supported on TiO_2. Additionally, UV-vis-NIR DRS electronic spectroscopy results indicated that in the oxide precursors, more defective Mo oxidic particles in stronger interaction with the support are formed on alumina than on titania. Since the alumina-supported catalyst is better promoted, as the IR-CO results indicated, it was postulated that the lower promotion of CoMo supported on titania compared to $CoMo/Al_2O_3$ has a structural origin and that the highly defective Mo oxide-phase structure supported on alumina facilitates the incorporation of the promoter into the crystalline lattice of MoS_2. This finding is in line with the differences in MoS_2 structure predicted by DFT theory when the support changes from alumina to titania [28]

since an edge-on MoS_2 structure found on TiO_2 would be more difficult to promote than a flat defective structure on the alumina surface.

It is clear that the value of the specific hydrodesulfurization rate constant (per gram of catalyst) for MoS_2 catalysts supported on different oxides is the result of several contributions that affect not only the edge dispersion of the MoS_2 particles but also the intrinsic activity of the different catalytic sites. The choice of the support matrix is therefore a key parameter in the preparation of highly active HDS catalytic materials since its nature can affect the performance of the different active sites in the catalyst. Moreover, it can affect the dispersion, the sulfidation, and the redox process of the supported phases during catalyst preparation and under HDS reaction conditions.

4.2.1 Catalyst Support Materials for Hydrodesulfurization of FCC Gasoline

Gasoline, one of the most widely used transport fuels, is a complex mix and in this way the gasoline pool receives contributions from a variety of refinery streams, including light straight run naphtha, isomerate, alkylate, FCC naphtha, and hydrocracker gasoline. Of these cuts, FCC naphtha is typically the largest volume component of the gasoline pool (30–40% v/v); moreover, FCC naphtha is responsible for about 80–95% of the total sulfur because it contains up to 2.5 wt% sulfur [29]. In contrast, the straight run naphtha, isomerate, and alkylate streams are very low in sulfur (<1 ppm S). Sulfur content is important because of environmental issues. Consequently, to achieve low sulfur content in the final fuel and meet environmental regulations like Tier 3 [30], the sulfur in the FCC naphtha incorporated to the gasoline pool must be reduced to 20–30 ppm. On the other hand, FCC naphtha contributes significantly to octane number due to its high content of olefins, up to 20 wt% [31], and aromatic compounds.

There are various process alternatives to decrease the sulfur content in FCC naphtha; among them one can either (a) pretreat the feed to the FCC unit, which is an expensive solution because of the high volume to pretreat, or (b) post-treat only the FCC product fraction that will be added to the gasoline pool (the so-called FCC naphtha).

The FCC naphtha fraction contains mainly thiophenic sulfur compounds of high reactivity and therefore, it is possible to attain during hydrotreatment sulfur levels below 10 ppm without great difficulty. In fact, it would be sufficient to operate at higher pressure and/or temperature to achieve low sulfur levels. However, under these more severe operating conditions, if allowed by thermodynamics, the hydrogenation reactions are enhanced and an important decrease in the olefin content, from 20 to 60 vol% to approximately 2 vol%, can take place, leading to a decrease of up to 10 octane numbers in the final gasoline [31]. Therefore, the key of this technology lies in the possibility to achieve high hydrodesulfurization (HDS)

minimizing the hydrogenation (HYD) reactions. There are two possibilities to solve this challenge: one is to understand the effect of the process variables, pressure (P), temperature (T), and liquid hourly space velocity (LHSV[1]). The other is the development of catalytic materials able to perform high hydrodesulfurization with minimum hydrogenation.

To analyze the possibility of obtaining low sulfur and high RON in the hydrodesulfurization of FCC naphtha, a laboratory study was conducted on the effects of changing the operating HDS conditions (T, P, LHSV) on the RON and sulfur content of the product, using a commercial $CoMoAl_2O_3$ catalyst, and a feed of stabilized FCC naphtha (original RON = 69) added with the proper amount of thiophene to reach 1000 ppm S. Both the experimental design and statistical analysis were performed using Statgraphics software.

A multiple response surface methodology and a Box-Behnken-type experimental design [32] were used to analyze two responses, the remaining sulfur content $(\overline{y}s)$ and the RON, as a function of three operating variables (factors in statistical nomenclature): LHSV = 3, 6, and 9 h^{-1}; temperature = 270, 300, and 330 °C; and pressure = 440, 480, and 520 psia leading to a total of 27 experiments. However, using the methodology Box-Behnken only 16 experiments were necessary to analyze the system.

In an attempt to illustrate the effect of three variables (LHSV, T, P) in a two-dimensional field, Fig. 4.2 shows an example of the effects obtained for each variable when the other two remain constant.

To help understand the effect of T, P, and LHSV, on the process, a surface response analysis was made by building a piecewise desirability function (δ) that expresses the desirable response for a combination of the process variables as a value of one if the response achieves some fixed desirable value. In this case, $\delta = 1$ if less than 30 ppm of sulfur is achieved in the processed naphtha: an intermediate value between 0 and 1 if the response factor is in the interval 1000–30 S ppm, and a value of zero if the response is equal or greater than the initial value. A maximization was used for the RON whereas a minimization was established for the remaining sulfur content in the product.

(a) For RON maximization, a loss of four RON units was considered acceptable with a RON lower limit of 65. In this case, the desirability function (δ) was defined as

$$\delta = \begin{cases} 0 & \text{if } \overline{y} \text{ does not reach } RON_{LL} \\ \left[\dfrac{\overline{y} - RON_{LL}}{RON^0 - RON_{LL}} \right] & \text{if } RON_{LL} \leq \overline{y} \leq RON^0 \\ 1 & \text{if } \overline{y} \geq RON^0 \end{cases}$$

---

[1] LHSV is the ratio of the hourly volume of oil processed to the volume of catalyst.
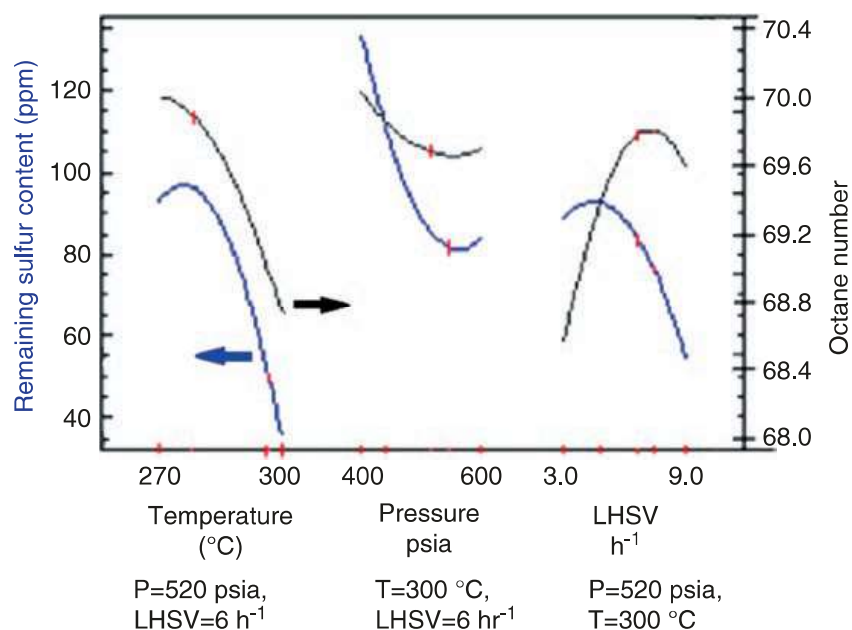
Fig. 4.2 Effect of temperature, pressure, and LHSV on the sulfur content (blue) and RON (black) after the hydrotreating of stabilized FCC naphtha with 1000 ppm S

where $\bar{y}$ is the RON after HDS processing, RON_{LL} is the lower acceptable RON limit, and RON^0 is the initial RON (in this case RON = 69).

(b) For the minimization of the remaining sulfur content ($\bar{y}$ s), considering 1000 ppm of S in the feed and setting the desirable lower limit of sulfur (S_{LL}) at 30 ppm. In consequence, the desirability function (δ) was defined as

$$\delta = \begin{cases} 1 & \text{if } \bar{y}\text{s is lower than } S_{LL} \\ \left[\dfrac{\bar{y}\text{s} - S^0}{S_{LL} - S^0}\right] & \text{if } S_{LL} \leq \bar{y}\text{s} \leq S^0 \\ 0 & \text{if } \bar{y}\text{s} \geq S^0 \end{cases}$$

where ($\bar{y}$ s) is the product sulfur content after HDS processing and S^0 is the initial sulfur concentration in ppm.

An optimization for the responses under the operating variables was made with the restrictions that the process must reach at least: RON >65, and S content <30 ppm. The best performance was obtained at LHSV = 6.75 h^{-1}. Using this fixed LHSV, the surface response for RON and remaining product sulfur was obtained for the different values of *T* and *P* (see Fig. 4.3).

The results of this example show that with a conventional CoMo HDS catalyst it is not possible, through the optimization of the operating conditions, to comply with the sulfur specification of 30 ppm S, maintaining simultaneously a desirable high octane number.

Fig. 4.3 Surface responses for the desirability function (δ) with respect to RON (blue) and remaining sulfur content (black), at LHSV of 6.75 h⁻¹, on the HDS of stabilized naphtha with 1000 ppm of sulfur
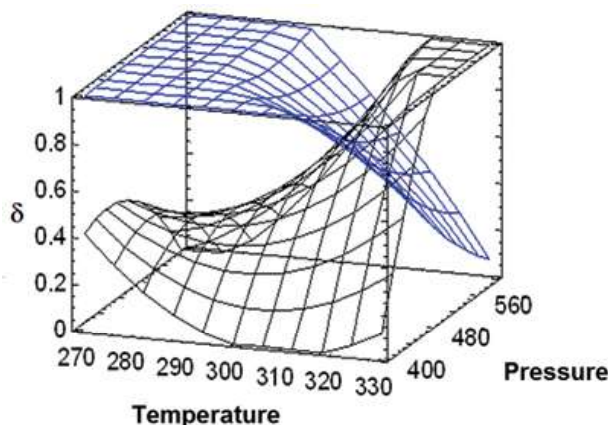
Therefore, a complete solution to the issue of obtaining clean FCC gasoline with high RON needs both the optimization of the process variables and the developing of hydrodesulfurization catalytic materials with high HDS/HYD selectivity ratio. To this end, several studies have been made in the past using catalysts with basic support matrixes to inhibit the transport of hydrogen and achieve HDS/HYD selectivity ratios higher than those obtained with active phases supported on alumina.

In an early study, Shimada et al. [33] analyzed the effect of using CoMo catalysts supported on MgO on the activity for hydrocracking (HYC) diphenylmethane. With MgO being a basic support the observed decrease in hydrocracking activity was an expected result. Nonetheless, an interesting result was that the MgO-supported catalyst showed a significant decrease in the hydrogenation activity. In another work, the same group confirmed this result using 1-methyl-naphthalene as reactant [17].

However, MgO in dry conditions has a surface area of around 200 m²/g but is a highly hygroscopic material and in the presence of water it is easily transformed into $Mg(OH)_2$, which has a low surface area of about 2 m²/g, and is therefore not a good matrix support for the HDS catalyst. Several approaches have been used in the preparation of HDS catalytic materials to compensate this problem: (i) producing MgO with high surface area [34], or (ii) using nonaqueous preparation methods to avoid the hydration of MgO [35]. However, such preparations are more expensive. A third approach has been to use a catalyst support matrix different from MgO, over which magnesia can be grafted or dispersed.

Supports of magnesia grafted on the surface of alumina were also investigated with the hypothesis that the hygroscopic behavior of pure magnesia could be avoided once magnesia is bonded to alumina through Mg-O-Al bridges. This approach hopes to preserve the high surface area provided by alumina.

Figure 4.4a shows the behavior of NiMo catalysts supported on alumina modified with different amounts of magnesia (NiMo/MgO(x)/Al₂O₃), where x = monolayers of MgO. It should be noted that the NiMo active phase chosen for this study presents a stronger hydrogenating function than the most suitable CoMo formulation. Catalysts were tested on two different reactions at atmospheric pressure: thiophene hydrodesulfurization and cyclohexene hydrogenation. The results showed that addition of magnesia to alumina produced a strong decrement in cyclohexene

Fig. 4.4 NiMo/Mg(X)-Al$_2$O$_3$: (**a**) activity for thiophene HDS (•) and cyclohexene HYD (▲); (**b**) selectivity ratio HDS of thiophene/HYD cyclohexene. Atmospheric pressure, differential continuous reactor. Theoretical MgO monolayer estimated as 2 OHs per Mg^{2+}
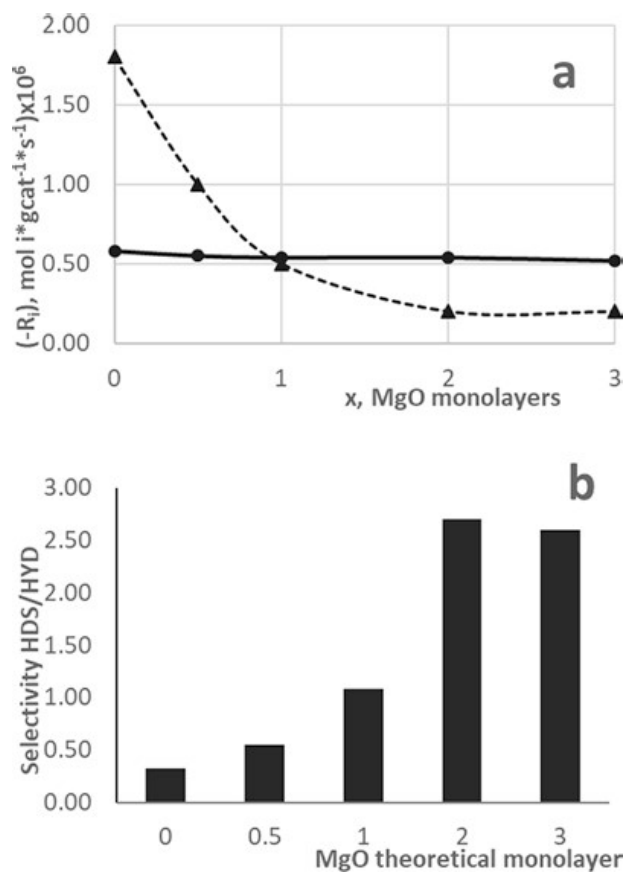
hydrogenation while the HDS of thiophene presented only a slight decrement. The decrement in the hydrogenation reaction was five times higher than the decrement of the desulfurization reaction, leading to an improved HDS/HYD ratio (Fig. 4.4b).

For NiMo catalysts supported on Al$_2$O$_3$–MgO mixed oxides with different x = MgO/MgO + Al$_2$O$_3$ molar ratios (0.0, 0.05, 0.25, 0.5, 0.75, and 1.0) [36], textural stability to the presence of water and high HDS/HYD ratio were found by Solis et al. [37] for low MgO contents (<0.25% mol). The catalysts however displayed a tendency to form nickel molybdate and NiO–MgO solid solution, taking away a significant amount of the Ni necessary to promote the MoS$_2$ phase.

Magnesium is not the only additive that confers basic properties. The possibility of modifying the alumina support with alkaline oxides has also been investigated. The addition of Li or K oxides to the alumina support of commercial catalysts caused a decrease in the hydrogenation and hydrodesulfurization activities. However, as in the case of magnesia, the decrease in HDS was less pronounced, leading to an improved HDS/HYD selectivity [38]. The addition of barium to the alumina support also caused the same behavior, a decrease in both rates of HDS and HYD but with an increase in the HDS/HYD selectivity [39]. In contrast, Miller et al. [40] reported no effect on the activity or HDS/HYD selectivity with addition of Ce to MoS$_2$/Al$_2$O$_3$ or K to CoMo/Al$_2$O$_3$. Likewise, supports of different kinds as hydro-

talcites have been used with success to improve the HDS/HYD selectivity ratio during the hydrodesulfurization of cracked naphtha [41].

Although the addition of alkaline earth oxides like MgO to alumina improves the HDS/HYD selectivity ratio, a decrease in the HDS activity is also caused to some extent because the Ni or Co promoters can form a stable phase with the support matrix. To overcome this problem, the combined use of alkaline-earth oxides as basic additives, heteropolycompounds as active-phase precursors containing Mo and Ni or Co promoter, and chelating agents to avoid the interaction of the Ni or Co promoter with the support matrix has been analyzed. Trejo et al. [42] used an aqueous impregnation with a chelating agent (CyDTA) to preserve or improve the HDS activity in CoMo catalysts supported on alumina modified with different amounts of MgO. The combination of potassium, citric acid, and a heteropolyacid, $H_3PMo_{12}O_{40}$, was also used in the preparation of selective $KCoMoP/Al_2O_3$ catalysts for the hydrotreating of FCC gasoline [43, 44].

Although several industrial processes based on catalysts with high HDS/HYD selectivity are offered (ScanFinning by Exxon-Mobil or Prime G by Axens), the research in this field continues since more restrictive environmental regulations are expected in the near future.

4.3   Improving HDS Catalytic Materials with the Use of Chelating Organic Additives

Alumina is widely used as a support for industrial hydrodesulfurization (HDS) catalysts of Co(Ni)-promoted molybdenum sulfide. The current challenge is to improve the alumina-supported catalysts in order to fulfill the requirements of production of clean transportation fuels [1, 19, 45]. The use of organic additives such as chelating agents during the preparation of Co(Ni)Mo HDS catalysts helps to improve their catalytic performance; according to literature, the use of a chelating agent during the catalyst preparation can lead to an increase in the number of Co(Ni)MoS promoted sites in the final catalyst [46–48]. It has been explained that the interaction of the chelating agent with the promoter produces a stable complex that sulfides at temperatures similar or higher than those required to sulfide oxidic Mo, facilitating the formation of the mixed Co(Ni)MoS phase and minimizing the formation of isolated phases of Ni or Co sulfide [49–52]. According to these results, the use of a chelating agent results in an enhanced promotion. However, a more detailed explanation of the effect of a chelating agent is convenient to better understand the characteristics of the active sites and to enable further improvements of the catalytic systems. It is not the purpose of this section to make a review of all chelating agents used in the preparation of HDS catalyst, but to make instead a detailed analysis of the effect of two chelating agents (ethylenediaminetetraacetic acid -EDTA- and citric acid -CA-) in Mo and CoMo HDS catalysts, with the aim of thoroughly understanding which of the changes induced by the use of the chelating agent has a real influence on the HDS behavior.

The CoMoS phase model, extensively used to analyze and explain the catalytic properties of hydrodesulfurization catalysts, is very useful to achieve this goal. This model is supported by experimental results that revealed the presence of Co atoms in MoS_2 crystallites, that is, the CoMoS phase, and is now accepted that such structures govern the catalytic activity of promoted catalysts [53–55]. Recently, scanning tunneling microscopy (STM) experiments and density functional theory (DFT) were used to demonstrate that in the most stable CoMoS phase, Co substitutes Mo at the edges of MoS_2 particles [2, 4, 11, 56, 57]. Some important characteristics of the active phase are still a subject of debate, for example, the local structure of the cobalt atoms on the edges of the MoS_2 crystallites. Based on nuclear magnetic resonance (NMR) and X-ray absorption near edge structure (XANES) analysis of promoted catalysts supported on different materials, several local structures where the Co atoms are bonded to five and/or six sulfur atoms in the CoMoS phase have been proposed [58–64].

Controversially, the combination of experimental and theoretical techniques revealed that the coordination number of Co in the CoMoS phase can be four instead of five or six. In particular, based on experimental results using STM or FT-IR of CO combined with DFT calculations, it was proposed that the Co atoms that substitute Mo on the edges of MoS_2 crystallites are fourfold coordinated with either tetrahedral, pseudo-tetrahedral, or square planar structure depending on the sulfur coverage, type of substituted edge (S or Mo), and promotion degree [11, 57, 65, 66].

It is not surprising that the FT-IR of CO can provide experimental evidence to achieve such type of information of the catalytic materials. The IR analysis of adsorbed NO or CO probe molecules is a technique widely used to study unpromoted and promoted binding sites in HDS catalysts [67–70], including those prepared with organic additives such as the chelating agents, because the absorbance and features of the IR spectrum of the adsorbed molecule provide information on the amount and electronic characteristics of the binding sites. Several important issues in sulfided catalysts have been discussed with the IR analysis of probe molecules, sometimes in combination with other techniques. For example, IR studies of adsorbed NO with EXAFS showed that the adsorption sites are located in the MoS_2 edges instead of on the basal planes [71]. Better results were obtained with CO adsorption because it can distinguish Mo–S unpromoted sites from CoMoS promoted ones. On sulfided Mo/Al_2O_3 catalysts, Mo–S binding sites are associated with a strong band at 2110 cm^{-1} (Mo in Mo edge) with a weak, broad component at 2070 cm^{-1} (Mo in S edge). The intensity of the bands correlates well with the HDS activity of the unpromoted catalysts [72–74]. For sulfided $CoMo/Al_2O_3$ catalysts, a new strong band at 2070 cm^{-1}, which intensity is in line with the catalytic activity [75], corresponds to CO adsorbed on promoted sites.

The nature of the promoted sites (Mo or Co) and its local structure (tetrahedral, pseudo-tetrahedral, or square planar) is not clearly established by the features of the experimental IR spectrum alone. The information available from the spectrum is that the corresponding CO band on promoted sites appears at a different frequency, shifted from the bands corresponding to the adsorption on unpromoted Mo–S sites

(2110 cm^{-1}) and Co sites in cobalt sulfide (2094 cm^{-1}). DFT calculations were needed to propose the structures of the promoted sites mentioned above [65].

To improve the current supported catalysts it is important to know the local geometry of Co on the edges of the MoS$_2$ crystallites, to better understand and explain how the catalysts behave in reaction conditions. Even more important is to establish if the structure of Co has or not a significant impact on the catalyst activity. This is the subject of the following sections.

4.3.1 Effect of EDTA in the Electronic and Structural Characteristics of the CoMoS Site and Catalytic Performance of Co-promoted Mo/Al$_2$O$_3$ Catalysts

A detailed analysis of the FT-IR spectra of CO adsorbed on a series of catalysts (Mo/Al$_2$O$_3$, CoMo/Al$_2$O$_3$ (without EDTA) and CoMo-E/Al$_2$O$_3$ (using EDTA during preparation)) was useful to study the effect of the chelating agent EDTA in the promotion of CoMo catalysts [76].

It was observed that the absorbance of the peak of CO adsorbed on CoMoS sites (at ~2072 cm^{-1}) [76] in the IR spectra is bigger in CoMo-E/Al$_2$O$_3$, compared to the CoMo/Al$_2$O$_3$ catalyst (see Fig. 4.5). The evaluation of the number of sites and the absorption coefficient indicated that the more intense absorbance is not related to a greater amount of adsorbing sites, but instead to a bigger absorption coefficient in CoMo-E/Al$_2$O$_3$: ε_{CoMoS} (CoMo-E/Al$_2$O$_3$)/ε_{CoMoS} (CoMo/Al$_2$O$_3$) = 1.9 [76]. This result needed an interpretation of the CO spectra different to the traditional one, because

Fig. 4.5 IR spectra of CO adsorbed on sulfided catalysts at ~100 K and 1 Torr. (**a**) Mo/Al$_2$O$_3$, (**b**) CoMo/Al$_2$O$_3$, (**c**) CoMo-E/ Al$_2$O$_3$. Reprinted from [76] with permission from Elsevier
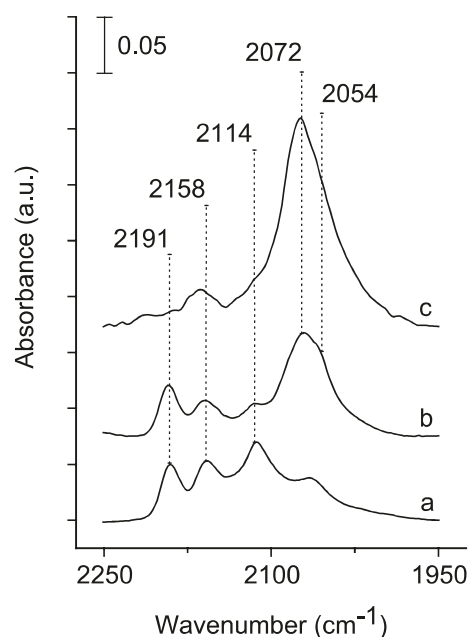
it was regularly assumed that at each CO vibration frequency on sulfided catalysts (at 2072 cm^{-1} in this case) corresponds to the same value of CO absorption coefficient.

The observed change in the magnitude of the absorption coefficients must arise from differences in the electronic interaction between the probe and the CoMoS adsorbing site. It was proposed in [76] that the CO absorption coefficient changes with the local structure of the surface atoms to which the probe is adsorbed.

The experimental fact that the absorption coefficient of CO adsorbed on CoMoS sites in CoMo/Al$_2$O$_3$ is different to that of CO adsorbed on CoMo-E/Al$_2$O$_3$ indicates that at least part of the surface where CO is adsorbed on the catalysts has metallic character or that sites with metallic character are in the vicinity of the CO-adsorbing sites [77]. Otherwise, no changes in absorbance could be detected. This inference of metallic character in MoS$_2$ crystallites can be well supported by repeated reports of the metallic character of cobalt-substituted edges and at the S layer at the top of MoS$_2$ crystallites, observed with STM experiments and explained by DFT calculations [57].

In the case of adsorption on metallic surfaces, the IR selection rule states that a vibrational mode will be IR active only if there is a nonzero projection of the dynamic dipole moment along the surface normal [78]. In other words, the magnitude of the absorption coefficient will depend on the inclination of the adsorbed molecule with respect to the surface normal. The effect is considered to apply to particles down to a few nanometers in size [79, 80], or even to metal carbonyl clusters [81], and has been observed in experiments performed in transmission IR spectroscopy [82, 83].

DFT calculations of different possible local structures of Co or Mo in Co-promoted MoS$_2$ crystallites showed that the fully promoted MoS$_2$ crystallite exposes cobalt atoms in fourfold coordination with tetrahedral structure in the S edge and square planar structure in the Mo edge [65]. For the non-fully promoted MoS$_2$ crystallite, where both Mo and Co are exposed on the edges, it was found that in the S edge Mo and Co are fourfold coordinated in tetrahedral structure and that in the Mo edge Mo is fourfold and fivefold coordinated, while Co is fourfold coordinated and presents pseudo-tetrahedral structure. That is, Mo and Co have a tetrahedral or pseudo-tetrahedral structure, except in the fully promoted Mo edges, where Co has a square planar structure.

The use of the chelating agent leads to higher promotion and presumably to higher proportion of CoMoS sites with Co in square planar structure in fully promoted Mo edges of the MoS$_2$ crystallite in CoMo-E/Al$_2$O$_3$ [76]. In this type of Co local structure the adsorption of CO can be perpendicular to the surface, resulting in an increased absorption coefficient, compared to a hindered adsorption in Co or Mo with tetrahedral or pseudo-tetrahedral local structure that projects a smaller part of the dynamic dipole into the surface normal. Then, the increased absorption coefficient in CoMo-E/Al$_2$O$_3$ can be related to a bigger proportion of Co in a square planar local structure in the better promoted catalyst [76].

In this interpretation of an experimental fact (the increased absorption coefficient with the use of EDTA as chelating agent) an important issue of the IR analysis of CO adsorbed on Co-promoted molybdenum catalysts is revealed: the correct quantification of adsorption sites requires the proper assignation of the absorption coefficient for each catalyst.

It is important to highlight that the analysis of CO adsorbed on the several possible structures of the CoMoS sites provided by DFT calculations allowed to understand that the Co atom is the adsorption site, and that as the promotion is enhanced with the use of EDTA as chelating agent more Co in square planar local structure is found in the surface of the MoS_2 crystallites.

The effect of this change in local structure, consequence of the addition of EDTA, in the catalytic activity was analyzed with the HDS of thiophene, dibenzothiophene, and 4,6-dimethyl dibenzothiophene [76]. TOF values are presented in Table 4.1.

The ratio (TOF of CoMoS)/(TOF of MoS) indicated that the addition of EDTA does not have a significant effect on the HDS of thiophene or DBT, meaning that the change in local structure to square planar in the catalysts prepared with EDTA does not have an impact on the HDS of thiophene or DBT: these molecules are transformed independently of the local structure of the promoted site. In the case of 4,6-DMDBT, the TOF's ratio changes with the use of EDTA, from 5.2 in CoMo-E/Al_2O_3 to 4.4 in CoMo/Al_2O_3. Apparently, with this sterically hindered molecule, the change from tetrahedral and/or pseudo-tetrahedral to the open square planar structure induced by the use of a chelating agent as EDTA has a positive effect on the hydrodesulfurization of 4,6-DMDBT.

In summary, the IR analysis of adsorbed CO indicates that the use of EDTA as chelating agent during preparation induces changes in the structure of the CoMoS sites in supported catalysts. These changes have no effect on the TOF of thiophene or DBT, while a positive one is observed in the case of 4,6-DMDBT.

Table 4.1 Turnover frequency for the HDS reaction of S-containing molecules

		$TOF \times 10^2$ (Mo–S site, s^{-1})	$TOF \times 10^2$ (Co–Mo–S site, s^{-1})	$\dfrac{TOF_{Co-Mo-S}}{TOF_{Mo-S}}$
4,6-DMDBT	Mo	0.11	–	–
	CoMo	–	0.49	4.4
	CoMo-E	–	0.58	5.2
DBT	Mo	0.23	–	–
	CoMo	–	4.02	17.1
	CoMo-E	–	4.18	17.7
T	Mo	3.26	–	–
	CoMo	–	91.7	28.1
	CoMo-E	–	91.3	28.0

Taken from [76] with permission from Elsevier

4.3.2   Effect of Citric Acid in the Characteristics and Catalytic Performance of Non-promoted and Co-promoted Molybdenum HDS Catalyst

The use of chelating agents in the preparation of Mo-based catalysts can lead to other modifications in the characteristics of the active phase (besides that in the structure of the CoMoS sites with the use of EDTA explained above), such as the sulfidation extent, edge dispersion, amount of adsorbing sites, level of promotion, and stacking of MoS_2 crystallites [84, 85]. It is important to understand if the changes in the active phase have a significant impact on the HDS catalytic activity. The study of the effect of citric acid (CA) in alumina-supported unpromoted and Co-promoted Mo catalysts was used to analyze which of the changes induced by the presence of the chelating agent have more influence on the HDS catalytic activity. To this end, two series of catalysts with increasing amounts of CA (CA/metal = 0, 1, and 2) were prepared, one of unpromoted Mo catalysts (Mo–CA(0)/Al_2O_3, Mo–CA(1)/Al_2O_3, and Mo–CA(2)/Al_2O_3), and a second one of catalyst promoted with Co (CoMo–CA(0)/Al_2O_3, CoMo–CA(1)/Al_2O_3, and CoMo–CA(2)/Al_2O_3). The calcination step during preparation was avoided to preserve the effect of the organic agent until sulfidation. For comparison, two calcined catalysts were prepared (Mo/Al_2O_3 and CoMo/Al_2O_3) [86].

The effect of CA on the amount and nature (MoS or CoMoS) of adsorbing sites was studied with infrared spectroscopy of adsorbed CO. The results in Table 4.2 show that CA causes a slight decrease in number of adsorbing sites in the case of unpromoted catalysts. In contrast, in the case of Co-promoted catalysts the use of CA has two important consequences: (a) the amount of total adsorbing sites (MoS and CoMoS) is strongly increased, mainly due to an approximately fourfold enlargement of CoMoS sites; (b) in the catalysts prepared with CA, the proportion of CoMoS site is increased: in CoMo–CA(1)/Al_2O_3 and CoMo–CA(2)/Al_2O_3 almost all adsorbing sites are promoted ones.

It is observed in Table 4.3 that the absorption coefficients of catalysts prepared without citric acid are small (21.7 ± 3.7 cm µmole^{-1}) compared with those of cata-

Table 4.2 Amount (µmole/g_{cat}) and percentage of active sites in sulfided catalysts evaluated with FT-IR of adsorbed CO

	Mo–S sites	Co–Mo–S sites	Total sites
Mo/Al_2O_3	155	–	155
Mo–CA(0)/Al_2O_3	170	–	170
Mo–CA(1)/Al_2O_3	110	–	110
Mo–CA(2)/Al_2O_3	118	–	118
CoMo/Al_2O_3	62 (47.7%)	68 (52.3%)	130
CoMo–CA(0)/Al_2O_3	37 (26.4%)	103 (73.6%)	140
CoMo–CA(1)/Al_2O_3	10 (5.4%)	175 (94.6%)	185
CoMo–CA(2)/Al_2O_3	11 (4.2%)	253 (95.8%)	264

Taken from [86] with permission from Elsevier

Table 4.3 Absorption coefficients (cm μmole⁻¹) of CO adsorbed on sulfided catalysts

	ε of Co–Mo–S sites
CoMo/Al$_2$O$_3$—(2067 cm⁻¹)	24.3
CoMo–CA(0)/Al$_2$O$_3$—(2067 cm⁻¹)	19.1
CoMo–CA(1)/Al$_2$O$_3$—(2067 cm⁻¹)	32.8
CoMo–CA(2)/Al$_2$O$_3$—(2067 cm⁻¹)	27.9

Extracted from [86] with permission from Elsevier

lysts prepared with CA (30.4 ± 3.5 cm μmole⁻¹). As in the case of catalysts prepared with EDTA, the absorption coefficient of CO for CoMoS sites increases in the catalysts prepared with CA even though the vibration frequency of CO remains at 2067 cm⁻¹, suggesting differences in the local structure of Co in the CoMoS site. The increase in the absorption coefficient of adsorbed CO can be explained through a greater proportion of fully promoted Mo edges in the MoS$_2$ crystallites with Co in square planar structure. In contrast, the lower absorption coefficient of CO in catalysts prepared without CA indicates that CO is adsorbed on Co with tetrahedral or pseudo-tetrahedral structures, present in partially promoted Mo edges and also in S edges.

The sulfidation extent is also affected by the presence of CA in the catalyst preparation. From temperature-programmed sulfidation experiments (TPS) of catalysts sulfided at 10 K/min, it was found that the total S/Mo ratio increases from 1.3 and 1.0 in Mo/Al$_2$O$_3$ and Mo–CA(0)/Al$_2$O$_3$ to S/Mo ratios of 2.1 and 2.2 for Mo–CA(1)/Al$_2$O$_3$ and Mo–CA(2)/Al$_2$O$_3$, respectively. Also in Co-promoted catalysts, the S/(Mo + Co) ratio increases from 1.0 and 0.7 in CoMo/Al$_2$O$_3$ and CoMo–CA(0)/Al$_2$O$_3$ to 1.7 and 2.0 for CoMo–CA(1)/Al$_2$O$_3$ and CoMo–CA(2)/Al$_2$O$_3$. Temperature-programmed reduction of sulfide experiments (TPR-S) also pointed to a better sulfidation of unpromoted and Co-promoted catalysts with CA. In the reduction patterns of unpromoted and Co-promoted molybdenum sulfide (see Fig. 4.6 for TPR-S patterns of promoted catalysts), the reduction of stoichiometric MoS$_2$ begins at 452 K and continues until 1233 K. At the final temperature of the experiment the reduction is still in progress, but the S/Mo ratio in the case of unpromoted catalysts and the S/(Mo + Co) ratio in the case of promoted ones increase with the CA content (Table 4.4). These results evidence that the introduction of CA during the preparation of the catalysts induces a better sulfidation.

Using the TPR-S experiments, the value of $\Delta H°$ of reduction of MoS$_2$ in the catalysts can be calculated from a plot of $1/T$ versus ln[H$_2$S], like the one presented in Fig. 4.7 [87]. The results, reported in Table 4.4, showed that the introduction of Co renders the MoS$_2$ crystallite more defective and therefore more reducible in surface and bulk in catalysts with and without CA.

As explained above, several characteristics of the Mo-based catalysts change with the addition of an organic agent as CA. Their catalytic performance was evaluated in the HDS of DBT and 4,6-DMDBT to identify which of the changes is important to the activity. DBT is a good choice to probe the level of promotion of MoS$_2$

Fig. 4.6 TPR-S patterns of promoted sulfided catalysts. (**a**) CoMo/Al$_2$O$_3$, (**b**) CoMo–CA(0)/Al$_2$O$_3$, (**c**) CoMo–CA(1)/Al$_2$O$_3$, (**d**) CoMo–CA(2)/Al$_2$O$_3$. Reprinted from [86] with permission from Elsevier
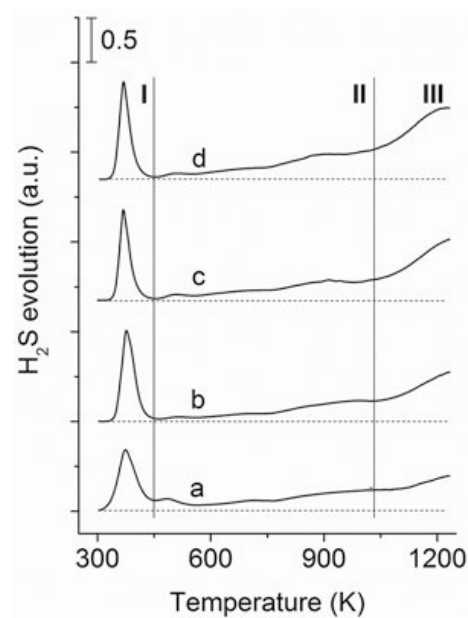
**Table 4.4** S/Mo, S/(Mo + Co) ratios, and ΔH°_{red} from TPR-S experiments

	S/Mo, S/(Mo + Co) (II + III)	ΔH°_{red} (kJ/g at S)
Mo/Al$_2$O$_3$	0.5	79
Mo–CA(0)/Al$_2$O$_3$	0.4	70
Mo–CA(1)/Al$_2$O$_3$	0.9	71.5
Mo–CA(2)/Al$_2$O$_3$	1.4	70
CoMo/Al$_2$O$_3$	0.7	46
CoMo–CA(0)/Al$_2$O$_3$	0.8	64
CoMo–CA(1)/Al$_2$O$_3$	1.0	68
CoMo–CA(2)/Al$_2$O$_3$	1.3	60

The enthalpy of reduction was calculated from the H$_2$S evolution in region III. Extracted from [86] with permission from Elsevier

crystallites, since it is transformed through the hydrogenation route as well as the direct desulfurization one over unpromoted MoS$_2$, while in the promoted catalysts the former is predominant. The measurement of activity in the 4,6-DMDBT molecule helps to evaluate if the changes induced by the use of CA have an influence on the HDS of refractory molecules that occur mainly through the hydrogenating path [88].

Table 4.5 reports the results of rate constants in both HDS reactions. In the case of unpromoted catalysts, no significant increase is observed in the rate constants with the presence of CA in the HDS of DBT. The TOF values (obtained from the measurement of the number of adsorption sites in the IR analysis of CO) are small

Fig. 4.7 Plot of $\ln[H_2S]$ versus $1/T$ of the TPR-S pattern of CoMo–CA(2)/ Al$_2$O$_3$. The linearization in 1034–1206 K is pointed out by the dotted straight line. Reprinted from [86] with permission from Elsevier
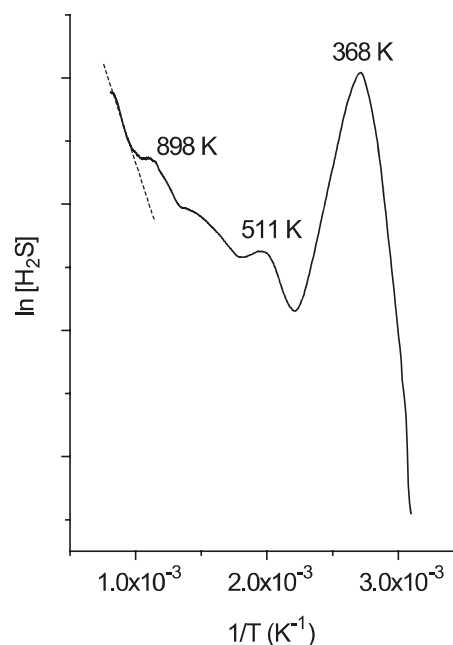
Table 4.5 Turnover frequency (TOF) and rate constant for the HDS of dibenzothiophene

	Rate constant $\times\ 10^1$ (cm^3 g$_{Mo+Co}^{-1}$ s^{-1})	TOF $\times\ 10^2$ (Mo–S sites, s^{-1})	TOF $\times\ 10^2$ (Co–Mo–S sites, s^{-1})
Mo/Al$_2$O$_3$	0.81	0.14	–
Mo–CA(0)/ Al$_2$O$_3$	1.2	0.18	–
Mo–CA(1)/ Al$_2$O$_3$	1.0	0.26	–
Mo–CA(2)/ Al$_2$O$_3$	1.2	0.29	–
CoMo/Al$_2$O$_3$	5.9	–	2.7
CoMo–CA(0)/ Al$_2$O$_3$	8.1	–	2.2
CoMo–CA(1)/ Al$_2$O$_3$	11.6	–	2.3
CoMo–CA(2)/ Al$_2$O$_3$	15.3	–	2.1

Taken from [86] with permission from Elsevier

for the unpromoted catalysts and do not considerably change with the use of citric acid. This means that the modifications induced by citric acid, as the increase of the sulfidation extent, have little or no effect on the catalytic activity of the MoS site. On the contrary, the incorporation of CA in promoted catalysts leads to an approximately threefold increase in the rate constant. However, the change in the TOF value is not significant. The result indicates that the change in the local structure from mainly tetrahedral (catalysts with no CA) to mainly square planar (catalysts with CA)

Table 4.6 Turnover frequency (TOF) and rate constant (k) for the HDS of 4,6-dimethyldibenzothiophene

	$k \times 10^1$ (cm^3 g$_{Mo+Co}^{-1}$ s^{-1})	TOF $\times 10^2$ (Mo–S sites, s^{-1})	TOF $\times 10^2$ (Co–Mo–S sites, s^{-1})
Mo/Al$_2$O$_3$	0.96	0.17	–
CoMo/Al$_2$O$_3$	1.1	–	0.38
CoMo–CA(1)/Al$_2$O$_3$	2.1	–	0.41
CoMo–CA(2)/Al$_2$O$_3$	2.5	–	0.33

Taken from [86] with permission from Elsevier

and the greater sulfidation extent induced by CA have little influence on the intrinsic activity of the catalytic site. Therefore, the increase in the rate constant with CA is related to an increase in the number of promoted active sites.

The incorporation of Co to the MoS$_2$ phase does not significantly change the HDS activity in 4,6-DMDBT. However, the use of CA duplicates the rate constant (Table 4.6). The fact that the TOF does not change considerably with the incorporation of the promoter or with the addition of CA indicates that the higher sulfidation level of the catalysts prepared with CA, which favors the formation of the more hydrogenating type II and brim active sites, does not affect substantially the intrinsic activity of the catalytic site.

In conclusion, these two examples show that both EDTA and CA induce changes in the sulfided catalysts. The IR analysis of adsorbed CO in catalysts prepared with and without EDTA showed that the absorption coefficient is not the same in both cases, revealing that the electronic structure is different. It was proposed that the local structure of Co in the edges of the MoS$_2$ crystallite changes with the use of EDTA. The same was observed in catalysts prepared with CA, but this is not the only characteristic that may be modified with the use of a chelating agent. The study of promoted and unpromoted catalysts prepared with CA was useful to understand that the increase in the rate constant with CA is related to an increase in the number of promoted active sites, and that the other characteristics that change with the use of the chelating agent, as the Co local structure and sulfidation extent, have less influence on the catalytic behavior of sulfided catalysts.

4.4   Co(Ni)-Mo(W)-Based Heteropolycompounds as Catalyst Precursors

The synthesis of highly active hydrodesulfurization catalysts depends significantly on the level of promotion reached during catalyst preparation. To achieve a higher number of promoted Co(Ni)-Mo(W)-S sites, it is desirable for the Co(Ni) and Mo(W) atoms to be as close as possible during the activation step of the catalyst. An interesting alternative to achieve this is the use of a single precursor salt that

already contains in its structure both atoms, Mo(W) and Co(Ni), in the desired ratio, instead of using two different salt precursors, one for Mo(W) and one for Co(Ni), as in the conventional HDS catalyst preparation procedure. Several experimental works concerning the use of Mo(W) heteropolycompounds (HPC) with different structures as precursor salts for the preparation of HDS catalysts are reported in the scientific literature.

In a recent review, Nikulshin et al. [89] and references therein reported the use of several polyoxometalate structures to prepare hydrotreatment catalysts: Lindqvist $[M_xM'_{6-x}O_{19}]^{(2+x)-}$, Keggin $[XM_{12}O_{40}]^{n-}$, Anderson $[XM_6O_{24}H_6]^{n-}$, Dawson $[X_2M_{18}O_{62}]^{n-}$, Strandberg $[X_2M_5O_{23}]^{n-}$, or Waugh $[Ni_9MoO_{32}]^{6-}$, where M(M') is a metallic cation and X is a nonmetallic one. However, the most frequently used heteropolymolybdates (heteropolytungstates) for the preparation of catalysts for deep HDS are heteropolyacids with Keggin, Dawson, or Anderson structures, and their Co(Ni) salts [90, 91].

Alumina-supported catalysts synthesized using polyoxometalate structures have mainly been evaluated in the HDS of thiophene and dibenzothiophene [92, 93], and some catalysts supported on mesoporous silica (HMS) have been tested in the HDS of dibenzothiophene [94] and only a few in the HDS of a refractory compound like 4,6-DMDBT or real mixtures such as straight run gas oil (SRGO) or a mixture of SRGO with LCGO [95]. In all cases whatever the polyoxometalate structure used to prepare the catalyst, the performance was better than for similar catalysts prepared from conventional precursors such as ammonium heptamolybdate and nickel or cobalt nitrate.

One of the drawbacks of the use of heteropolycompounds as impregnating salts for the preparation of HDS catalysts is the low stoichiometric Co(Ni)/Mo atomic ratio, which is below the optimal value (0.49) reported for catalysts synthesized using conventional precursors. Some authors have used reduced Keggin-type HPCs to increase the stoichiometric Co(Ni)/Mo ratio from 0.125 to 0.29. In laboratory tests of the hydrodesulfurization of thiophene and 4,6-DMDBT HDS, catalysts prepared with heteropolycompounds showed conversions 10 and 29% higher than their counterparts prepared using conventional precursors, respectively. The higher HDS activity of the catalysts prepared with HPCs was related to an increment in the number of Co-promoted molybdenum sites produced by the close interaction between cobalt and molybdenum in the Keggin structure during the catalyst activation (sulfidation) process [92, 96].

Recently, the optimal Co/Mo ratio has been achieved using a cobalt salt of the dimer $Co_2Mo_{10}O_{39}H_4^{6-}$ with Anderson structure as impregnating precursor for CoMo catalysts supported on alumina, titania, and zirconia and tested in the HDS of thiophene. For all the CoMo catalysts, whatever the support, the best performance was obtained for those prepared with the cobalt salt of the $Co_2Mo_{10}O_{39}H_4^{6-}$ dimer [97]. The superior performance of the catalyst prepared with the dimer was related to the higher dispersion achieved with this preparation method, and to the better cobalt promotion associated to the preservation of the Anderson structure during the catalyst preparation.

4.4.1   Stability of the Supported Polyoxometalate Structure

4.4.1.1   Stability During Support Impregnation

An important aspect to be considered, during the catalyst synthesis, is the stability of the heteropolyacid (HPA) or heteropolycompound (HPC) during the impregnation of the support. Several materials have been used to support both types of precursors (HPA and HPC), and their thermal stability depends on the surface characteristics of the support matrix and on the metallic load. Greater stability is achieved when the HPC is impregnated on a support matrix with an isoelectric point (IEP) ≤ 7, for example, on titania [98], silica [97], or silica-containing mesoporous materials like MCM-41 [99] and SBA-15 [100]. For alumina- and zirconia-supported catalysts where the support IEP is >7, the HPA structure is not preserved after impregnation due to the stronger interaction between the electronegative molybdophosphate anions and the electropositive Zr and Al cations, which contribute first to its distortion and then to its breakdown during the impregnation process [94]. To overcome this problem, Griboval et al. [101] proposed the use of a cobalt salt of the reduced Keggin HPA for the preparation of cobalt-promoted alumina-supported HDS catalysts. The preservation of the HPA molecular structure after impregnation was corroborated by Raman and NMR analysis. The higher stability of the reduced salt at a pH value near the isoelectric point of the alumina support (IEP = 8) avoids the interaction of cobalt atoms with the support, preventing the formation of the inactive $CoAl_2O_4$ spinel, allowing for a higher number of cobalt atoms to be available for the formation of the active CoMoS mixed phase, as demonstrated in [70].

In another work, Ramírez et al. [96] used a less interacting support like SBA-15 with 0–15 wt% of titanium oxide grafted on the surface to prepare NiMoP HDS catalysts, using phosphomolybdic acid and nickel citrate as precursors for the active phase. The use of the heteropolyacid led to catalysts with higher HDS activity in the HDS of 4,6-DMDBT than those prepared conventionally with ammonium heptamolybdate, nickel nitrate, and phosphoric acid. The observed changes in catalytic activity were related to a twofold increase in the activity of the catalytic sites. Additionally, it was found that grafting TiO_2 to the surface of the SBA matrix stabilizes and preserves the ordered structure of the latter during the calcination process, and the structure of the heteropoly anion in the impregnation step [92].

4.4.1.2   Stability Under Thermal Treatment

The preparation of HDS catalysts with MoS_2 structures well promoted by Co or Ni requires to maintain the Ni(Co) and Mo elements close to each other. Therefore, the structure of the heteropolycompound must be preserved up until the catalyst is activated by sulfidation. The calcination of the active-phase precursor salts, which is normally applied before activating the catalyst by sulfidation, must be avoided when

using heteropolycompounds as active-phase precursors since this step is detrimental to the structure of the HPC and therefore to the promotion and final performance of the catalyst, as reported by Romero-Galarza et al. [70] for alumina-supported CoMoP catalysts. For the case of CoMoP HDS catalysts prepared by impregnating alumina with an aqueous solution of a reduced heteropolycompound with Keggin structure, $Co_{7/2}PMo_{12}O_{40}$, Fig. 4.8 reveals that the catalytic activity of the uncalcined catalyst was 1.33 times higher than the calcined one. This effect was related to a higher number of Co-promoted molybdenum sites that were quantified by CO adsorption experiments (Table 4.7).

In summary, the improvement in HDS activity when using polyoxometalate structures as precursors for the synthesis of Co(Ni)Mo hydrotreatment catalysts is related to maintaining stable the structure of the heteropolyoxometalate up until the activation step in order to achieve high promotion of the molybdenum species after the sulfidation process. The good performance of the HDS catalysts prepared with polyoxometalate structures can be explained because molybdenum and cobalt(nickel)

Fig. 4.8 Pseudo first-order reaction rate constants for dried (CoMoP/Al-D) and calcined CoMoP/Al catalysts. HDS of 4,6-DMDBT at T = 320 °C and 1200 psig of hydrogen. D = dried catalyst, 350 and 400 are the calcination temperatures in Celsius degrees. Adapted from [70] with permission of Elsevier
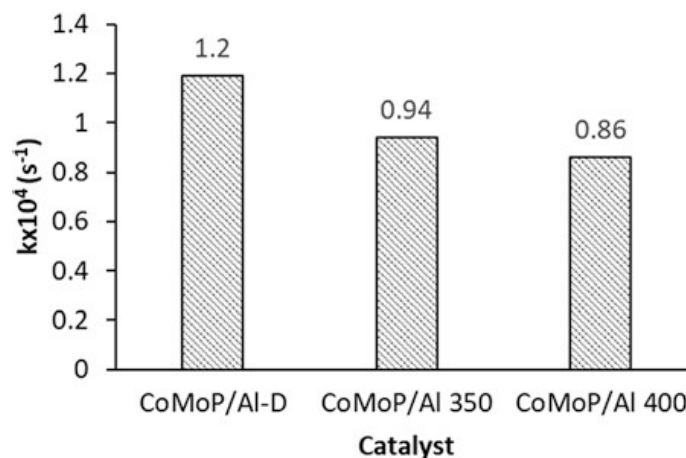
Table 4.7 Quantitative analysis from CO adsorption experiments and pseudo first-order rate constants for CoMoP/Al catalysts prepared at different calcination temperatures

Catalyst	$k \times 10^4$ (s^{-1})	Mo sites 2110 cm^{-1} (mol/g$_{cat}$) $\times 10^5$	CoMo sites 2070 cm^{-1} (mol/g$_{cat}$) $\times 10^5$	Total sites (mol/g$_{cat}$) $\times 10^5$
CoMoP/ Al-D	1.19	2.6	3.6	6.2
CoMoP/ Al350	0.94	3.0	2.7	5.7
CoMoP/ Al400	0.86	1.7	2.0	3.7
CoAHM/ Al400	0.47	1.8	1.6	3.4

HDS of 4,6-DMDBT after 6 h of reaction at T = 320 °C and 1200 psig of hydrogen. D = dried catalyst, 350 and 400 are the calcination temperatures in Celsius degrees. *AHM* Ammonium heptamolybdate

Extracted from [70] with permission of Elsevier

are part of the same compound structure, and this avoids the formation of inactive phases formed by the interaction of the promotor atoms with the support framework, and favors the formation of a greater number of promoted sites in the Co(Ni)–Mo–S nanoclusters.

4.5 Sulfidation Methodology

The final step in the preparation of supported hydrodesulfurization catalysts is the transformation of the active-phase oxide precursors into sulfides. The operating conditions at which the sulfidation process takes place have crucial importance in the active-phase morphology and catalytic performance as shown by several authors [1, 102–106].

The sulfidation of the oxide catalyst precursors can lead to two different types of promoted structures in CoMo/Al$_2$O$_3$ catalysts named "type I" and "type II." "Type I" structure displays low HDS activity and is typical of molybdenum sulfide interacting with the alumina support through Mo-O-Al bridges. The other structure called "type II" has high HDS activity and is obtained when the sulfidation of the oxide precursor is complete, and Mo and Al are not bonded.

Most of the studies on sulfidation have been made at laboratory scale, with sulfidation usually carried out flowing a gaseous stream of H$_2$S/H$_2$ through the catalyst bed at atmospheric pressure and temperatures ranging from 573 to 723 K. In contrast, industrial sulfidation involves the use of high pressures and liquid sulfiding agents (i.e., dimethyl disulfide) [107, 108], where also temperature and H$_2$S concentration gradients in the catalyst bed must be accounted for in the sulfidation procedure [109].

The sulfidation-reduction of supported Mo oxide species supported on alumina to produce supported MoS$_2$ is well known and has been studied by several authors [102, 110–112]. The first systematic study of the sulfidation of MoO$_3$ supported on alumina was made by Arnoldy et al. [110] (see Fig. 4.9).

In general, the sulfidation-reduction process can follow two transformation routes: (a) oxygen-sulfur exchange in Mo^{6+} oxide species followed by reduction, or (b) reduction of Mo oxide species followed by sulfidation as Fig. 4.9 shows. The O → S exchange (I) in Mo^{6+} species is an easy process that takes place without change in the structure, and occurs at temperatures lower than 500 K. In this process, the reaction consumes H$_2$S and releases water. The reduction of partially or fully exchanged species consumes hydrogen and releases H$_2$S. The suggested route for the sulfidation of hydrodesulfurization catalyst is to achieve first full sulfidation of the Mo^{6+} species at low temperatures and then increase the temperature to reduce MoS$_3$ to MoS$_2$.

The reduction of oxide Mo^{6+} to Mo^{4+} species involves a change of structure and occurs at higher temperatures, consuming H$_2$ and producing water. The subsequent sulfidation of reduced Mo^{4+} oxide species is not easy and may be at the origin of the presence of partially sulfided species of low activity in the final catalyst.
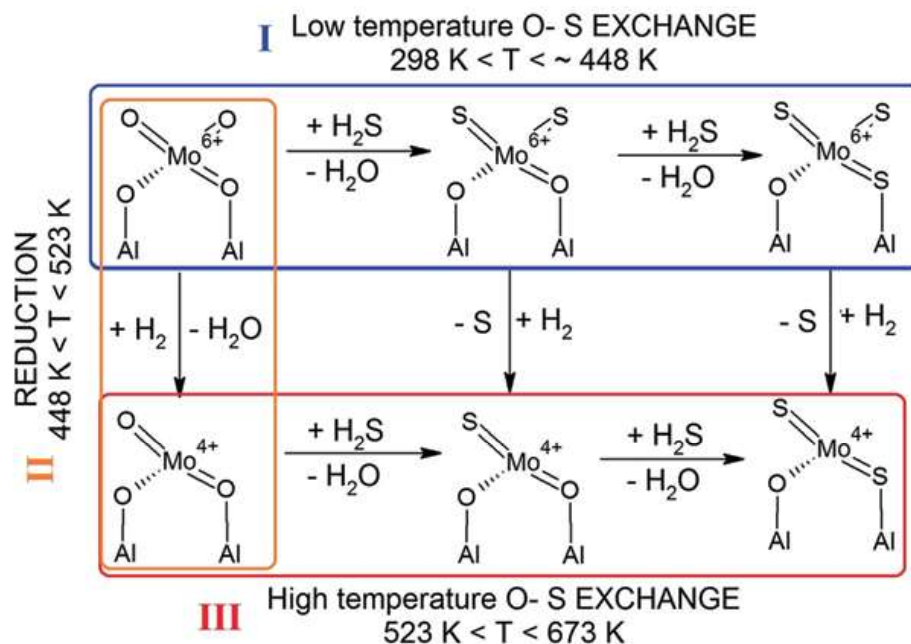
Fig. 4.9 Sulfidation paths for supported MoO_3/Al_2O_3. Adapted from [110] with permission from Elsevier

According to literature [111], better levels of sulfidation are achieved when the major part of the H_2S consumption takes place before Mo^{6+} is converted into Mo^{4+} [113]. Arnoldy et al. suggested that full exchange of oxygen by sulfur in Mo^{6+} species at low temperatures can be achieved by using a low heating rate (1 K/min) during sulfidation. This will give time to do the exchange of oxygen by sulfur at the lower temperatures and then, at the higher temperatures reached at the end of the heating ramp, perform the reduction of Mo^{6+} to Mo^{4+}. This is especially relevant since strong support interactions and small particle size could slow down the sulfidation kinetics of Mo and Ni [114, 115].

During temperature-programmed reduction or sulfidation (TPR or TPRS) experiments carried out to analyze the reduction or sulfidation behavior of the supported species, it must be considered that the reduction or sulfidation peaks associated to the different species can overlap significantly due to the presence of highly defective surface species making difficult the interpretation of the thermogram traces.

With the aim of studying the role of the sulfidation process in the case of hydrodesulfurization catalysts prepared with or without an organic additive (citric acid), Villarreal et al. [116] prepared and tested $NiMo/SiO_2/Al_2O_3$ hydrodesulfurization catalysts using/or not citric acid as additive and 4 wt% SiO_2 grafted on γ-Al_2O_3 as support. The use of citric acid can increase the level of promotion, reduce the metal-support interaction, and enhance the hydrogenation/desulfurization selectivity due to the better sulfidation of the catalysts [84, 86, 112, 114, 117–119]. To investigate the effect of the sulfidation heating ramp on the catalyst activity and selectivity, $NiMo/SiO_2/Al_2O_3$ catalysts prepared with or without citric acid (CA) were tested in

the hydrodesulfurization of 4,6-DMDBT using different rates of heating during sulfidation (1, 3, 10 K/min), as displayed in Fig. 4.10.

As shown in Fig. 4.10, the catalysts with and without citric acid (CA/NiMo and NiMo) increase their HDS activity when the sulfidation heating ramp is slow. For the catalyst with citric acid the activity increased 100% when the heating ramp went from 10 to 1 K/min. Furthermore, the effect of the slow heating rate was higher when citric acid was used because the slower heating rate avoided the rapid decomposition of the organic and preserved the metal dispersion [86, 120, 121].

Using temperature-programed sulfidation (TPS) it was possible to evaluate the consumption of H_2S (Table 4.8). For both catalysts, with and without citric acid, the amount of H_2S consumed before the main peak of H_2S production was greater when slow heating rates were used.
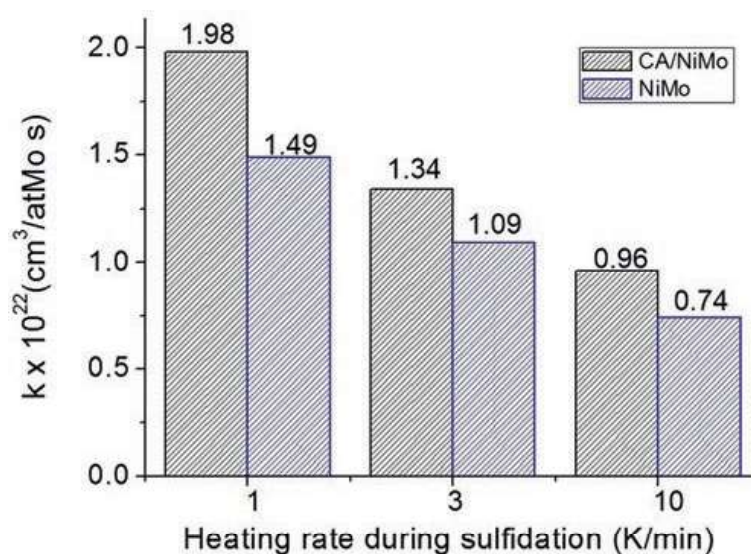
Fig. 4.10 Catalytic activity of NiMo/SiO$_2$/Al$_2$O$_3$ and CA/NiMo/SiO$_2$/Al$_2$O$_3$ in the HDS of 4,6-DMDBT (593 K and 1200 PSI) previously sulfided in a flow of H_2S/H_2 (15% vol.) at 673 K heating at 1, 3, and 10 K/min. Reprinted from [116] with permission from Elsevier

Table 4.8 H_2S consumption, and sulfidation levels (S/Mo) for NiMo/SiO$_2$/Al$_2$O$_3$ and CA/NiMo/SiO$_2$/Al$_2$O$_3$ catalyst

	Heating rate during sulfidation (K/min)	H_2S consumption (mmols)[a]	S/Mo atomic ratio[a]
NiMo/SiO$_2$/Al$_2$O$_3$	1	0.41	1.73
	3	0.32	1.36
	10	0.15	0.64
CA/NiMo/SiO$_2$/Al$_2$O$_3$	1	0.41	1.75
	3	0.38	1.64
	10	0.33	1.43

[a]Calculated at the end of the TPS experiment
Adapted from [116] with permission from Elsevier

These results show that although the sulfidation is not complete, a slower rate of heating leads to better sulfidation levels and improved catalytic activity, probably because it favors the sulfidation of Mo^{6+} species before its reduction to Mo^{4+}. Accordingly, the catalysts sulfided with a slow heating rate consume the most part of H_2S at low temperatures. Oxysulfidic species, resulting from partial sulfidation, are difficult to sulfide and are known as type I species with low HDS activity [114, 122].

To study the effect of the sulfidation methodology in NiMo catalysts prepared from Keggin heteropolyacids supported on alumina grafted with 4 wt% TiO_2 or SiO_2 (TiO_2/Al_2O_3 or SiO_2/Al_2O_3), the catalysts were sulfided in one or two steps using in all cases a heating ramp of 1 K/min and the following temperature programs: (a) 673 K for 4 h, (b) 563 K for 4 h, and (c) a first plateau at 423 K for 2 h followed by a second plateau at 563 K for 3 h. After sulfidation, the activity of these catalysts was tested in the HDS of 4,6-DMDBT.

The pseudo first-order reaction rate constants and the individual hydrogenation and direct desulfurization rate constants are presented in Table 4.9. Sulfiding directly from ambient to 673 K is the worst procedure leading to lower global activities and also lower hydrogenation and direct desulfurization individual rate constants. The best procedure seems to be the use of a two-temperature-step sulfidation. In this case, regardless of the support, the global activity is the highest.

Low-temperature sulfidation or sulfiding in two steps seems to increase slightly the hydrogenation rate constant. In contrast, clear increases in the direct desulfurization constant are observed when sulfiding at lower temperature or in two steps. In the analysis of these results, no account was taken of the changes in dispersion caused by the different sulfidation temperatures.

The above results indicate that to obtain more active HDS catalysts it is convenient to establish a sulfidation procedure that allows the largest exchange of S in the low-temperature region, before reducing Mo. This will enhance the sulfidation of the catalyst and the formation of more active type II catalytic sites, leading to a higher activity, particularly when the catalysts are prepared using organic additives, such as citric acid [86, 115, 118, 123–125].

Table 4.9 Rate constants (k) in the HDS of 4,6-DMDBT (593 K and 1200 PSI), catalysts were sulfided in a flow of H_2S/H_2 (15% vol.)

Catalyst	Sulfidation program	$k \times 10^{22}$ cm^3/at Mo–s	k_{HYD} cm^3/at Mo–s	k_{DDS} cm^3/at Mo–s
NiMoP/TiO$_2$/Al$_2$O$_3$	(a) 673 K, 4 h	0.83	0.65	0.18
	(b) 563 K, 4 h	1.10	0.89	0.21
	(c) 423 K, 2 h; 563 K, 3 h	1.24	0.84	0.40
NiMoP/SiO$_2$/Al$_2$O$_3$	(a) 673 K, 4 h	0.59	0.52	0.07
	(b) 563 K, 4 h	0.70	0.57	0.13
	(c) 423 K, 2 h; 563 K, 3 h	0.80	0.60	0.20

4.6   Final Comments

The performance of supported hydrodesulfurization catalysts is highly sensitive to the preparation method. Important improvements in activity and selectivity can be achieved through the selection of the catalyst support, the use of organic additives, and the use of different precursor salts, particularly heteropolycompounds that include in their structure the adequate ratio of Co(Ni) to Mo. It is also clear that the procedure used for activating hydrodesulfurization catalysts by sulfidation can substantially change the catalyst performance. The use of a slow heating ramp (1 K/min) or several ramps during the sulfidation procedure can help to achieve higher extents of sulfidation and consequently more active catalysts.

Hydrogenation and hydrodesulfurization reactions take place at different active sites located in different parts of the active-phase nanoparticle. Therefore, the particle morphology influences the activity and hydrogenation/desulfurization selectivity of the catalysts. Thus, careful attention must be paid to the consequences of changing the catalyst preparation procedure since, given the different nature of the desulfurization and hydrogenation active sites, a change that benefits one type of site can be deleterious to the other. Generally, a combination of strategies is required to achieve high-performing HDS catalysts.

References

1. H. Topsøe, B.S. Clausen, F.E. Massoth, Hydrotreating catalysis, in *Catalysis*, ed. by A. J. R. Boudart, M., (Springer-Verlag, Berlin Heidelberg New York, 1996), pp. 1–269. https://doi. org/10.1007/978-3-642-61040-0_1
2. L.S. Byskov, J.K. Nørskov, B.S. Clausen, H. Topsøe, DFT calculations of unpromoted and promoted MoS_2-based hydrodesulfurization catalysts. J. Catal. **187**, 109–122 (1999). https:// doi.org/10.1006/jcat.1999.2598
3. P. Raybaud, J. Hafner, G. Kresse, S. Kasztelan, H. Toulhoat, Ab Initio study of the H_2–H_2S/ MoS_2 gas–solid interface: the nature of the catalytically active sites. J. Catal. **189**, 129 (2000). https://doi.org/10.1006/jcat.1999.2698
4. P. Raybaud, J. Hafner, G. Kresse, S. Kasztelan, H. Toulhoat, Structure, energetics, and electronic properties of the surface of a promoted MoS_2 catalyst: an ab initio local density functional study. J. Catal. **190**, 128–143 (2000). https://doi.org/10.1006/jcat.1999.2743
5. H. Schweiger, P. Raybaud, G. Kresse, H. Toulhoat, Shape and edge sites modifications of MoS_2 catalytic nanoparticles induced by working conditions: a theoretical study. J. Catal. **207**, 76–87 (2002). https://doi.org/10.1006/jcat.2002.3508
6. H. Schweiger, P. Raybaud, H. Toulhoat, Promoter sensitive shapes of Co(Ni)MoS nanocatalysts in sulfo-reductive conditions. J. Catal. **212**, 33–38 (2002). https://doi.org/10.1006/ jcat.2002.3737
7. S. Cristol, J.F. Paul, E. Payen, D. Bougeard, S. Clémendot, F. Hutschka, Theoretical study of the MoS_2 (100) surface: a chemical potential analysis of sulfur and hydrogen coverage. 2. Effect of the total pressure on surface stability. J. Phys. Chem. B **106**, 5659–5667 (2002). https://doi.org/10.1021/jp0134603

8. M.V. Bollinger, K.W. Jacobsen, J.K. Nørskov, Atomic and electronic structure of MoS$_2$ nanoparticles. Phys. Rev. B **67**, 085410 (2003). https://doi.org/10.1103/PhysRevB.67.085410

9. B. Hinnemann, J.K. Nørskov, H. Topsøe, A density functional study of the chemical differences between type I and type II MoS$_2$-based structures in hydrotreating catalysts. J. Phys. Chem. B **109**, 2245–2253 (2005). https://doi.org/10.1021/jp048842y

10. S. Helveg, J.V. Lauritsen, E. Laegsgaard, I. Stensgaard, J.K. Nørskov, B.S. Clausen, H. Topsøe, F. Besenbacher, Atomic-scale structure of single-layer MoS$_2$ nanoclusters. Phys. Rev. Lett. **84**, 951–954 (2000). https://doi.org/10.1103/PhysRevLett.84.951

11. J.V. Lauritsen, S. Helveg, E. Lægsgaard, I. Stensgaard, B.S. Clausen, H. Topsøe, F. Besenbacher, Atomic-scale structure of Co-Mo-S nanoclusters in hydrotreating catalysts. J. Catal. **197**, 1–5 (2001). https://doi.org/10.1006/jcat.2000.3088

12. A.K. Tuxen, H.G. Füchtbauer, B. Temel, B. Hinnemann, H. Topsøe, K.G. Knudsen, F. Besenbacher, J.V. Lauritsen, Atomic-scale insight into adsorption of sterically hindered dibenzothiophenes on MoS$_2$ and Co–Mo–S hydrotreating catalysts. J. Catal. **295**, 146–154 (2012). https://doi.org/10.1016/j.jcat.2012.08.004

13. Á. Logadóttir, P.G. Moses, B. Hinnemann, N.Y. Topsøe, K.G. Knudsen, H. Topsøe, J.K. Nørskov, A density functional study of inhibition of the HDS hydrogenation pathway by pyridine, benzene, and H$_2$S on MoS$_2$-based catalysts. Catal. Today **111**, 44–51 (2006). https://doi.org/10.1016/j.cattod.2005.10.018

14. R. Candia, O. Sørensen, J. Villadsen, N.-Y. Topsøe, B.S. Clausen, H. Topsøe, Effect of sulfiding temperature on activity and structures of Co-Mo/Al$_2$O$_3$ catalysts. II. Bull. Soc. Chim. Belg. **93**, 763–773 (1984). https://doi.org/10.1002/bscb.19840930818

15. J. Ramirez, S. Fuentes, G. Díaz, M. Vrinat, M. Breysse, M. Lacroix, Hydrodesulphurization activity and characterization of sulphided molybdenum and cobalt-molybdenum catalysts. Comparison of alumina-, silica-alumina- and titania-supported catalysts. Appl. Catal. **52**, 211–224 (1989). https://doi.org/10.1016/S0166-9834(00)83385-0

16. J. Ramírez, F. Sánchez-Minero, Support effects in the hydrotreatment of model molecules. Catal. Today **130**, 267–271 (2008). https://doi.org/10.1016/j.cattod.2007.10.103

17. H. Shimada, T. Sato, Y. Yoshimura, J. Hiraishi, A. Nishijima, Support effect on the catalytic activity and properties of sulfided molybdenum catalysts. J. Catal. **110**, 275–284 (1988). https://doi.org/10.1016/0021-9517(88)90319-3

18. M. Breysse, J.L. Portefaix, M. Vrinat, Support effects on hydrotreating catalysts. Catal. Today **10**, 489–505 (1991). https://doi.org/10.1016/0920-5861(91)80035-8

19. A. Stanislaus, A. Marafi, M.S. Rana, Recent advances in the science and technology of ultra low sulfur diesel (ULSD) production. Catal. Today **153**, 1–68 (2010). https://doi.org/10.1016/j.cattod.2010.05.011

20. H. Shimada, Morphology and orientation of MoS$_2$ clusters on Al$_2$O$_3$ and TiO$_2$ supports and their effect on catalytic performance. Catal. Today **86**, 17–29 (2003). https://doi.org/10.1016/S0920-5861(03)00401-2

21. J. Ramirez, L. Cedeño, G. Busca, The role of titania support in Mo-based hydrodesulfurization catalysts. J. Catal. **184**, 59–67 (1999). https://doi.org/10.1006/jcat.1999.2451

22. J. Ramírez, G. Macías, L. Cedeño, A. Gutiérrez-Alejandre, R. Cuevas, P. Castillo, The role of titania in supported Mo, CoMo, NiMo, and NiW hydrodesulfurization catalysts: analysis of past and new evidences. Catal. Today **98**, 19–30 (2004). https://doi.org/10.1016/j.cattod.2004.07.050

23. L. Coulier, J.A.R. van Veen, J.W. Niemantsverdriet, TiO$_2$-supported Mo model catalysts: Ti as promoter for thiophene HDS. Catal. Lett. **79**, 149–155 (2002). https://doi.org/10.1023/A:1015312509749

24. C. Arrouvel, M. Breysse, H. Toulhoat, P. Raybaud, A density functional theory comparison of anatase (TiO$_2$)- and γ-Al$_2$O$_3$-supported MoS$_2$ catalysts. J. Catal. **232**, 161–178 (2005). https://doi.org/10.1016/j.jcat.2005.02.018

25. P. Castillo-Villalón, J. Ramírez, R. Cuevas, P. Vázquez, R. Castañeda, Influence of the support on the catalytic performance of Mo, CoMo, and NiMo catalysts supported on Al$_2$O$_3$

and TiO$_2$ during the HDS of thiophene, dibenzothiophene, or 4,6-dimethyldibenzothiophene. Catal. Today **259**, 140–149 (2015). https://doi.org/10.1016/j.cattod.2015.06.008

26. R.R. Chianelli, G. Berhault, P. Raybaud, S. Kasztelan, J. Hafner, H. Toulhoat, Periodic trends in hydrodesulfurization: in support of the Sabatier principle. Appl. Catal. A Gen. **227**, 83–96 (2002). https://doi.org/10.1016/S0926-860X(01)00924-3

27. J. Ramírez, A. Gutierrez-Alejandre, Characterization and hydrodesulfurization activity of W-based catalysts supported on Al$_2$O$_3$–TiO$_2$ mixed oxides. J. Catal. **170**, 108–122 (1997). https://doi.org/10.1006/jcat.1997.1713

28. D. Costa, C. Arrouvel, M. Breysse, H. Toulhoat, P. Raybaud, Edge wetting effects of γ-Al$_2$O$_3$ and anatase-TiO$_2$ supports by MoS$_2$ and CoMoS active phases: A DFT study. J. Catal. **246**, 325–343 (2007). https://doi.org/10.1016/j.jcat.2006.12.007

29. T.G. Kaufmann, A. Kaldor, G.F. Stuntz, M.C. Kerby, L.L. Ansell, Catalysis science and technology for cleaner transportation fuels. Catal. Today **62**, 77–90 (2000). https://doi.org/10.1016/S0920-5861(00)00410-7

30. P. Gripka, O. Bhan, W. Whitecotton, J. Esteban, Catalytic strategies to meet gasoline sulphur limits. Digit. Refining Process. Oper. Maintenance (2015). www.digitalrefining.com/article/1001120

31. C. Song, An overview of new approaches to deep desulfurization for ultra-clean gasoline, diesel fuel and jet fuel. Catal. Today **86**, 211–263 (2003). https://doi.org/10.1016/S0920-5861(03)00412-7

32. G.E.P. Box, J.S. Hunter, W.G. Hunter, *Statistics for Experimenters: Design, Innovation, and Discovery*, 2nd edn. (John Wiley & Sons, Inc., Hoboken, NJ, 2005)

33. H. Shimada, M. Kurita, T. Sato, Y. Yoshimura, T. Hirata, T. Konakahara, K. Sato, A. Nishihima, Support effect on the hydrocracking activity of molybdenum catalysts. Chem. Lett. **13**, 1861–1864 (1984). https://doi.org/10.1246/cl.1984.1861

34. T. Klicpera, M. Zdražil, High surface area MoO$_3$/MgO: preparation by the new slurry impregnation method and activity in sulphided state in hydrodesulphurization of benzothiophene. Catal. Lett. **58**, 47–51 (1999). https://doi.org/10.1023/A:1019036724583

35. T. Klicpera, M. Zdražil, Synthesis of a high surface area monolayer MoO$_3$/MgO catalyst in a (NH$_4$)$_6$Mo$_7$O$_{24}$/MgO/methanol slurry, and its hydrodesulfurization activity. J. Mater. Chem. **10**, 1603–1608 (2000). https://doi.org/10.1039/b001375g

36. T. Klimova, D. Solís Casados, J. Ramirez, New selective Mo and NiMo HDS catalysts supported on Al$_2$O$_3$-MgO(x) mixed oxides. Catal. Today **43**, 135–146 (1998). https://doi.org/10.1016/S0920-5861(98)00142-4

37. D. Solís, T. Klimova, J. Ramírez, T. Cortez, NiMo/Al$_2$O$_3$–MgO(x) catalysts: the effect of the prolonged exposure to ambient air on the textural and catalytic properties. Catal. Today **98**, 99–108 (2004). https://doi.org/10.1016/j.cattod.2004.07.024

38. D. Mey, S. Brunet, C. Canaff, F. Maugé, C. Bouchy, F. Diehl, HDS of a model FCC gasoline over a sulfided CoMo/Al$_2$O$_3$ catalyst: Effect of the addition of potassium. J. Catal. **227**, 436–447 (2004). https://doi.org/10.1016/j.jcat.2004.07.013

39. R. Zhao, C. Yin, H. Zhao, C. Liu, Effects of modified Co-Mo catalysts for FCC gasoline HDS on catalytic activity. Pet. Sci. Technol. **22**, 1455–1463 (2004). https://doi.org/10.1081/LPET-200027756

40. J.T. Miller, W.J. Reagan, J.A. Kaduk, C.L. Marshall, A.J. Kropf, Selective hydrodesulfurization of FCC naphtha with supported MoS$_2$ catalysts: the role of cobalt. J. Catal. **193**, 123–131 (2000). https://doi.org/10.1006/jcat.2000.2873

41. C. Sudhakar, Selective hydrodesulfurization of cracked naphtha using hydrotalcite-supported catalysts, Patent 5,851,382, 1998

42. F. Trejo, M. Rana, J. Ancheyta, CoMo/MgO–Al$_2$O$_3$ supported catalysts: an alternative approach to prepare HDS catalysts. Catal. Today **130**, 327–336 (2008). https://doi.org/10.1016/j.cattod.2007.10.105

43. P. Nikulshin, D. Ishutenko, Y. Anashkin, A. Mozhaev, A. Pimerzin, Selective hydrotreating of FCC gasoline over KCoMoP/Al$_2$O$_3$ catalysts prepared with H$_3$PMo$_{12}$O$_{40}$: Effect of metal loading. Fuel **182**, 632–639 (2016). https://doi.org/10.1016/j.fuel.2016.06.016

44. D. Ishutenko, P. Nikulshin, A. Pimerzin, Relation between composition and morphology of K(Co)MoS active phase species and their performances in hydrotreating of model FCC gasoline. Catal. Today **271**, 16–27 (2016). https://doi.org/10.1016/j.cattod.2015.11.025

45. D.D. Whitehurst, T. Isoda, I. Mochida, Present state of the art and future challenges in the hydrodesulfurization of polyaromatic sulfur compounds. Adv. Catal. **42**, 345–471 (1998). https://doi.org/10.1016/S0360-0564(08)60631-8

46. J.A.R. van Veen, E. Gerkema, A.M. van der Kraan, P.A.J.M. Hendriks, H. Beens, A ^{57}Co Mössbauer emission spectrometric study of some supported CoMo hydrodesulfurization catalysts. J. Catal. **133**, 112–123 (1992). https://doi.org/10.1016/0021-9517(92)90189-O

47. R. Cattaneo, F. Rota, R. Prins, An XAFS study of the different influence of chelating ligands on the HDN and HDS of γ-Al$_2$O$_3$-supported NiMo catalysts. J. Catal. **199**, 318–327 (2001). https://doi.org/10.1006/jcat.2001.3170

48. A.J. van Dillen, R.J.A.M. Terörde, D.J. Lensveld, J.W. Geus, K.P. de Jong, Synthesis of supported catalysts by impregnation and drying using aqueous chelated metal complexes. J. Catal. **216**, 257–264 (2003). https://doi.org/10.1016/S0021-9517(02)00130-6

49. M. Sun, D. Nicosia, R. Prins, The effects of fluorine, phosphate and chelating agents on hydrotreating catalysts and catalysis. Catal. Today **86**, 173–189 (2003). https://doi.org/10.1016/S0920-5861(03)00410-3

50. G. Kishan, J.A.R. van Veen, J.W. Niemantsverdriet, Realistic surface science models of hydrodesulfurization catalysts on planar thin-film supports: the role of chelating agents in the preparation of CoW/SiO$_2$ catalysts. Top. Catal. **29**, 103–110 (2004). https://doi.org/10.1023/B:TOCA.0000029792.45691.d4

51. M.S. Rana, J. Ramírez, A. Gutiérrez-Alejandre, J. Ancheyta, L. Cedeño, S.K. Maity, Support effects in CoMo hydrodesulfurization catalysts prepared with EDTA as a chelating agent. J. Catal. **246**, 100–108 (2007). https://doi.org/10.1016/j.jcat.2006.11.025

52. N. Frizi, P. Blanchard, E. Payen, P. Baranek, M. Reibeilleau, C. Dupuy, J.P. Dath, Genesis of new HDS catalysts through a careful control of the sulfidation of both Co and Mo atoms: Study of their activation under gas phase. Catal. Today **130**, 272–282 (2008). https://doi.org/10.1016/j.cattod.2007.10.109

53. C. Wivel, R. Candia, B.S. Clausen, S. Mørup, H. Topsøe, On the catalytic significance of a Co-Mo-S phase in Co-Mo/Al$_2$O$_3$ hydrodesulfurization catalysts: combined in situ Mössbauer emission spectroscopy and activity studies. J. Catal. **68**, 453–463 (1981). https://doi.org/10.1016/0021-9517(81)90115-9

54. H. Topsøe, B.S. Clausen, R. Candia, C. Wivel, S. Mørup, In situ Mössbauer emission spectroscopy studies of unsupported and supported sulfided Co-Mo hydrodesulfurization catalysts: evidence for and nature of a Co-Mo-S phase. J. Catal. **68**, 433–452 (1981). https://doi.org/10.1016/0021-9517(81)90114-7

55. N.-Y. Topsøe, H. Topsøe, Characterization of the structures and active sites in sulfided Co-Mo/Al$_2$O$_3$ and Ni-Mo/Al$_2$O$_3$ catalysts by NO chemisorption. J. Catal. **84**, 386–401 (1983). https://doi.org/10.1016/0021-9517(83)90010-6

56. P. Raybaud, Understanding and predicting improved sulfide catalysts: Insights from first principles modeling. Appl. Catal. A Gen. **322**, 76–91 (2007). https://doi.org/10.1016/j.apcata.2007.01.005

57. J.V. Lauritsen, J. Kibsgaard, G.H. Olesen, P.G. Moses, B. Hinnemann, S. Helveg, J.K. Nørskov, B.S. Clausen, H. Topsøe, E. Lægsgaard, F. Besenbacher, Location and coordination of promoter atoms in Co- and Ni-promoted MoS$_2$-based hydrotreating catalysts. J. Catal. **249**, 220–233 (2007). https://doi.org/10.1016/j.jcat.2007.04.013

58. M.J. Ledoux, O. Michaux, G. Agostini, P. Panissod, CoMo sulfide catalysts studies by metal solid NMR: the question of the existence of the chemical synergy. J. Catal. **96**, 189–201 (1985). https://doi.org/10.1016/0021-9517(85)90372-0

59. M.J. Ledoux, On the structure of cobalt sulfide catalysts. Catal. Lett. **1**, 429–431 (1988). https://doi.org/10.1007/BF00766202

60. S.M.A.M. Bouwens, J.A.R. van Veen, D.C. Koningsberger, V.H.J. de Beer, R. Prins, Extended X-ray absorption fine structure determination of the structure of cobalt in carbon-supported

Co and Co-Mo sulfide hydrodesulfurization catalysts. J. Phys. Chem. **95**, 123–134 (1991). https://doi.org/10.1021/j100154a028

61. S.M.A.M. Bouwens, F.B.M. van Zon, M.P. van dijk, A.M. van der Kraan, V.H.J. de Beer, J.A.R. van Veen, D.C. Koningsberger, On the structural differences between alumina-supported CoMoS type I and alumina-, silica-, and carbon-supported CoMoS type ii phases studied by XAFS, MES, and XPS. J. Catal. **146**, 375–393 (1994). https://doi.org/10.1006/jcat.1994.1076

62. J.T. Miller, C.L. Marshall, A.J. Kropf, (Co)MoS2/alumina hydrotreating catalysts: an EXAFS study of the chemisorption and partial oxidation with O_2. J. Catal. **202**, 89–99 (2001). https://doi.org/10.1006/jcat.2001.3273

63. M.W.J. Crajé, S.P.A. Louwers, V.H.J. de Beer, R. Prins, A.M. van der Kraan, E.X.A.F.S. An, Study on the So-Called "Co-Mo-S" phase in Co/C and Co-Mo/C, compared with a Mössbauer emission spectroscopy study. J. Phys. Chem. **96**, 5445–5452 (1992). https://doi.org/10.1021/j100192a048

64. L. van Haandel, G.M. Bremmer, E.J.M. Hensen, T. Weber, The effect of organic additives and phosphoric acid on sulfidation and activity of (Co)Mo/Al_2O_3 hydrodesulfurization catalysts. J. Catal. **351**, 95–106 (2017). https://doi.org/10.1016/j.jcat.2017.04.012

65. A. Travert, C. Dujardin, F. Maugé, E. Veilly, S. Cristol, J.F. Paul, E. Payen, CO adsorption on CoMo and NiMo sulfide catalysts: a combined IR and DFT study. J. Phys. Chem. B **110**, 1261–1270 (2006). https://doi.org/10.1021/jp0536549

66. Y. Zhu, Q.M. Ramasse, M. Brorson, P.G. Moses, L.P. Hansen, C.F. Kisielowski, S. Helveg, Visualizing the stoichiometry of industrial-style Co-Mo-S catalysts with single-atom sensitivity. Angew. Chem. Int. Ed. Engl. **53**, 10723–10727 (2014). https://doi.org/10.1002/anie.201405690

67. F. Maugé, J.C. Lavalley, FT-IR study of CO adsorption on sulfided Mo/Al_2O_3 unpromoted or promoted by metal carbonyls: titration of sites. J. Catal. **137**, 69–76 (1992). https://doi.org/10.1016/0021-9517(92)90139-9

68. N.-Y. Topsøe, A. Tuxen, B. Hinnemann, J.V. Lauritsen, K.G. Knudsen, F. Besenbacher, H. Topsøe, Spectroscopy, microscopy and theoretical study of NO adsorption on MoS_2 and Co–Mo–S hydrotreating catalysts. J. Catal. **279**, 337–351 (2011). https://doi.org/10.1016/j.jcat.2011.02.002

69. J. Ramirez, P. Castillo, L. Cedeño, R. Cuevas, M. Castillo, J.M. Palacios, A. López-Agudo, Effect of boron addition on the activity and selectivity of hydrotreating CoMo/Al_2O_3 catalysts. Appl. Catal. A Gen. **132**, 317–334 (1995). https://doi.org/10.1016/0926-860X(95)00166-2

70. A. Romero-Galarza, A. Gutiérrez-Alejandre, J. Ramírez, Analysis of the promotion of CoMoP/Al_2O_3 HDS catalysts prepared from a reduced H–P–Mo heteropolyacid Co salt. J. Catal. **280**, 230–238 (2011). https://doi.org/10.1016/j.jcat.2011.03.021

71. H. Topsøe, R. Candia, N.-Y. Topsøe, B.S. Clausen, On the state of the Co-Mo-S Model. Bull. Des Sociétés Chim. Belges. **93**, 783–806 (1984). https://doi.org/10.1002/bscb.19840930820

72. J.B. Peri, Computerized infrared studies of Mo/Al_2O_3 and Mo/SiO_2 catalysts. J. Phys. Chem. **86**, 1615–1622 (1982). https://doi.org/10.1021/j100206a028

73. J. Bachelier, M. Tilliette, M. Cornac, J.C. Duchet, J.C. Lavalley, D. Cornet, Sulfided Co-Mo/Al_2O_3 catalysts: carbon monoxide chemisorption and surface structures. Bull. Soc. Chim. Belg. **93**, 743–750 (1984). https://doi.org/10.1002/bscb.19840930816

74. B. Müller, A.D. van Langeveld, J.A. Moulijn, H. Knözinger, Characterization of sulfided Mo/Al_2O_3 catalysts by temperature-programmed reduction and low-temperature Fourier transform infrared spectroscopy of adsorbed carbon monoxide. J. Phys. Chem. **97**, 9028–9033 (1993). https://doi.org/10.1021/j100137a031

75. F. Maugé, A. Vallet, J. Bachelier, J.C. Duchet, J.C. Lavalley, Preparation, characterization, and activity of sulfided catalysts promoted by Co(CO)3NO thermodecomposition. J. Catal. **162**, 88–95 (1996). https://doi.org/10.1006/jcat.1996.0262

76. P. Castillo-Villalón, J. Ramirez, R. Castañeda, Relationship between the hydrodesulfurization of thiophene, dibenzothiophene, and 4,6-dimethyl dibenzothiophene and the local structure